AGU ADVANCING EARTH AND SPACE SCIENCES

Water Resources Research

RESEARCH ARTICLE
10.1029/2024WR038264

Constraining the Modern Hydrological Balance of Bear Lake, Utah-Idaho: Insights From Stable Isotopes ($\delta^{18}O$ and $\delta^{2}H$)

M. J. Custado[1,2], C. A. Gagnon[1,2], B. Belanger[3], N. Sekhon[1,2,4], J. Bernstein-Schalet[1,2], C. W. Kinsley[5], W. D. Sharp[5], J. L. Oster[3], and D. E. Ibarra[1,2]

[1]Department of Earth, Environmental, and Planetary Sciences, Brown University, Providence, RI, USA, [2]Institute at Brown University for Environment and Society, Brown University, Providence, RI, USA, [3]Department of Earth and Environmental Sciences, Vanderbilt University, Nashville, TN, USA, [4]Department of Geology, Occidental College, Los Angeles, CA, USA, [5]Berkeley Geochronology Center, Berkeley, CA, USA

Key Points:

- Stable isotopes ($\delta^{18}O$ and $\delta^{2}H$) can be used to estimate the flux of the components of a lake's hydrological balance, including evaporation
- Applying isotopic techniques in hydrology requires better constraints on atmospheric moisture-related parameters such as humidity
- Modern lake isotopic mass balance models can inform the interpretation of paleoclimatic records and future climate scenarios

Supporting Information:

Supporting Information may be found in the online version of this article.

Correspondence to:

M. J. Custado,
manuel_justin_custado@brown.edu

Citation:

Custado, M. J., Gagnon, C. A., Belanger, B., Sekhon, N., Bernstein-Schalet, J., Kinsley, C. W., et al. (2025). Constraining the modern hydrological balance of Bear Lake, Utah-Idaho: Insights from stable isotopes ($\delta^{18}O$ and $\delta^{2}H$). *Water Resources Research*, *61*, e2024WR038264. https://doi.org/10.1029/2024WR038264

Received 21 JUN 2024
Accepted 16 MAR 2025

Abstract Freshwater lakes are vital water resources, especially in the context of a changing climate. Supplementing existing hydrological methods to monitor lake levels may greatly improve resource management, particularly in drought-prone regions. In this study, we performed dual-isotope ($\delta^{18}O$ and $\delta^{2}H$) calculations to model the hydrological balance of Bear Lake, Utah-Idaho. The lake is a critical water resource and site for paleoclimate studies of the latest Pleistocene. Using the Craig-Gordon isotopic mass balance model, we simultaneously constrained unknown fluxes, including groundwater discharge and particularly evaporation, which is typically under-constrained due to inconsistencies across existing methods. Data from community databases and sampling campaigns in 2022 and 2023 were utilized to derive an evaporation rate of 2.18×10^{8} m^3/yr ($\pm 4.94 \times 10^{6}$ m^3/yr, 1σ using $\delta^{18}O$; $\pm 3.47 \times 10^{6}$ m^3/yr, 1σ using $\delta^{2}H$) at a calculated relative humidity of 0.62 above the lake. Detailed analysis of the sensitivity of the model revealed that parameters related to atmospheric moisture, particularly humidity and its isotopic composition, significantly influence evaporation estimates. Using carbonate-based isotope data, we leveraged this sensitivity to provide insights in the evaporation and humidity at Bear Lake during different time periods. This study shows the potential of using modern water isotopic composition to aid with interpreting carbonate-based paleoclimate data sets and informing current and future water resource management practices.

Plain Language Summary Lakes are critical water resources that sustain ecosystems, agriculture, and domestic and industrial activities. Climate change threatens the sustainability of lakes as a resource; therefore, monitoring processes that regulate lake volumes is essential. Existing monitoring methods have inherent disadvantages and biases that present challenges in quantifying processes and fluxes, particularly evaporation. Analysis of the stable isotopes of water ($\delta^{18}O$ and $\delta^{2}H$) can complement current monitoring efforts. Methods for determining the stable isotopic composition of water are continually improving in terms of ease of use and efficiency. This study used newly reported data, supplemented by published isotopic data from the Bear River watershed, to characterize modern lake processes, estimate evaporation rates, and provide insights into past and future environmental conditions. In doing so, we demonstrated the utility of using stable isotopes for water management and research.

1. Introduction

Lakes are natural resources that provide a multitude of ecosystem services vital for sustaining aquatic ecological balance (Cantonati et al., 2020; Dudgeon et al., 2006; Schindler & Scheuerell, 2002). Fluctuations in lake water storage reflect the impacts of human water management (e.g., Cooley et al., 2021). Additionally, the physical processes that maintain lake levels are typically sensitive to climate variations. Hence, shifts in the chemical and hydrological properties of a lake reflect past and present climate dynamics. Parameters such as water level, temperature, evaporation rates, and ice phenology have been demonstrated to respond to changing climate (Adrian et al., 2009; Wang et al., 2018; Woolway et al., 2020; Wurtsbaugh et al., 2017). Downstream impacts of fluctuating hydrological regimes include changes in the water quality of groundwater resources (Barbieri et al., 2023; Sharan et al., 2023).

Constraining the inflows and outflows to lake bodies, which include evaporation, precipitation, groundwater discharge, and streamflow, is important for gauging the impact of climate change on the availability of critical freshwater resources. Various methods to quantify water fluxes encompass in situ chemical and physical measurements, remote sensing techniques, and multiparametric models (Gronewold et al., 2020; Henderson-Sellers, 1986; Yin & Nicholson, 1998; G. Zhao & Gao, 2019; G. Zhao et al., 2022; B. Zhao et al., 2024). Although the response of these processes to climate varies among lakes, global-scale analysis over the last few decades has shown increasing evaporation rates driven by elevated lake surface temperatures and decreasing ice cover, posing challenges to future water security (Barnett et al., 2005; Wang et al., 2018; Woolway et al., 2020).

The stable isotope ratios of water ($\delta^{17}O$, $\delta^{18}O$, $\delta^{2}H$) can provide a more uniform metric for studying regional lake balance changes than in situ measurements of hydrologic fluxes. The δ notation signifies that the isotopic measurement is relative to a known reference standard, typically the Vienna Standard Mean Ocean Water (VSMOW) (Coplen et al., 1983). Spatiotemporal variations in the isotopic composition of surface waters reflect the integrated influence of its meteorological sources and subsequent phase changes (Bowen & Good, 2015; Bowen et al., 2019; Dee et al., 2023; Jasechko, 2019). Oxygen and hydrogen isotope-based calculations have been shown to adequately characterize lake processes at different spatial and temporal scales (Gibson, Birks, & Yi, 2016; Gibson, Birks, Yi, Moncur, & McEachern, 2016; Gibson et al., 1993, 2019; Gonfiantini, 1986; Haig et al., 2020; Jasechko et al., 2014; Jones et al., 2007; Longinelli et al., 2008; Russell & Johnson, 2006; Steinman, Rosenmeier, & Abbott, 2010; Steinman, Rosenmeier, Abbott, & Bain, 2010; Vystavna et al., 2021). This approach offers the advantage of assessing lake changes without biases introduced by, for example, the operability and location of measurement gauges (Haig et al., 2020).

The theoretical model of using stable isotopes to carry out lake mass balance calculations, particularly for constraining fractionation during evaporation, was proposed in the 1960s by Craig and Gordon (1965). The classic Craig-Gordon model has been used as a foundational basis to describe the mechanics of isotopic fractionation during the evaporation of open water bodies. Briefly, the model describes evaporation as a function of the surface water isotopic composition, the equilibrium and kinetic transport processes at play, and the gradient of atmospheric conditions, particularly humidity and isotopic composition of moisture above the lake. Craig and Gordon proposed a structure above the lake incorporating both liquid-air and laminar interfaces where equilibrium and kinetic transport occurs, respectively, and a turbulent region where evaporating vapor mixes with other moisture sources (Craig & Gordon, 1965; Gonfiantini, 1986). Gonfiantini et al. (2018) proposed a unified Craig-Gordon model that simultaneously takes into account different environmental parameters that affect evaporation.

Isotopic mass balance calculations are commonly carried out using a single isotope. However, discrepancies between evaporation flux estimates using $\delta^{18}O$ and $\delta^{2}H$ exist due to differences in the fractionation magnitude of each isotope during kinetic transport (Xiao et al., 2017; Xie et al., 2021). Yi et al. (2008) introduced a coupled approach, utilizing both $\delta^{18}O$ and $\delta^{2}H$ data to fulfill mass balance calculations. We expand on this method by constructing a system of equations that solve for relative humidity and unknown fluxes, such as evaporation and groundwater discharge, to constrain the isotopic mass balance in the study site. By examining the isotope systematics during the evaporation process, the sensitivity of the calculations to different parameters can be quantified. Supplementing new physical and isotopic data with what is available in the literature, Bear Lake serves as an excellent site to apply this approach.

1.1. Hydroclimatic Setting

Bear Lake, situated on the border of Utah and Idaho within the northeastern Great Basin, has served as a reservoir for irrigation, flood management, and hydropower since 1912 (Dean, 2009; Kaliser, 1972). Prior to this, the lake was disconnected from the Bear River, until an inlet canal was built that altered the hydrology of the lake (Dean et al., 2007; Lamarra et al., 1986). Hydrological records have demonstrated the lake's sensitivity to regional precipitation and temperature changes in the western United States (Dean et al., 2009). In addition to being a valuable modern water resource, the lake has been the subject of numerous paleoclimate studies. Isotopic records from Bear Lake sediment cores drilled in 2000 reveal 250,000 years of alternating balance-filled and over-filled conditions across glacial-interglacial cycles (Bright et al., 2006; Colman et al., 2006, 2009; Dean, 2009; Dean et al., 2006; Kaufman et al., 2009; Passey & Ji, 2019).

In this paper, we utilize a network of available $\delta^{18}O$ and $\delta^{2}H$ data sets throughout the Bear River watershed to assess the modern annual hydrological balance of Bear Lake. Taking advantage of a rich data set, a dual isotope

approach is employed to jointly constrain the isotopic mass balances for $\delta^{18}O$ and $\delta^{2}H$ by solving for humidity and unknown fluxes, particularly evaporation. This provides a more robust calculation over the use of single isotope systems. Continuous monitoring of evaporation at Bear Lake is limited; therefore, this study aims demonstrate the utility of monitoring the isotopic composition of the lake as a resource management tool. Additionally, we explore the sensitivity of the calculations to different parameters and its implications in studying past, present, and future climates. The relative sensitivities of $\delta^{18}O$ and $\delta^{2}H$ to different climate and isotopic variables will also be described. Leveraging previously published lake sediment data can give insights on the climate conditions at Bear Lake across different times.

The manuscript opens with a discussion of the theory and assumptions embedded in the equations used, followed by a description of the data sets and the climatic setting of Bear Lake. The results section then presents all data, along with the two phases of computations performed: (a) separate mass balance calculations for $\delta^{18}O$ and $\delta^{2}H$, and (b) a dual-isotope approach using a system of equations. This is followed by a discussion of the sensitivity of the calculations to different parameters. Lastly, the paper concludes by demonstrating the use of the isotopic mass balance model to infer climatic conditions at Bear Lake during different periods: the present, the last interglacial, the last glacial period, and potential future warming.

2. Theory and Assumptions

2.1. Lake Isotopic Mass Balance

The equations used for lake isotopic mass balance models have been described in detail by Gonfiantini (1986), Gibson, Birks, and Yi (2016), and Gibson, Birks, Moncur, and McEachern (2016). Adopting the conventions of both sources, the following text provides a brief overview of the method and general approach.

The water mass balance of a lake, assuming well-mixed and hydrological steady-state conditions, is expressed by the following equation:

$$\frac{dV}{dt} = 0 = I - Q - E \tag{1}$$

where V is the volume of the lake, dV/dt is the change in volume with respect to time, I and Q are the total water inflow and outflow, respectively, and E is evaporation (Craig & Gordon, 1965; Gibson, Birks, & Yi, 2016; Gibson, Birks, Yi, Moncur, & McEachern, 2016; Gonfiantini, 1986). For this study, calculations are made on annual time scales.

Stable isotopes of water are typically used to estimate evaporation by deriving the ratio of evaporation over total water inflow (X) following the equation below:

$$X = \frac{E}{I} = \frac{\delta_I - \delta_L}{\delta_E - \delta_L} \tag{2}$$

where δ_I, δ_E, δ_L are the isotopic composition (either $\delta^{18}O$ or $\delta^{2}H$, ‰) of the total water inflow, evaporated vapor, and the lake water, respectively (Craig & Gordon, 1965; Gibson, Birks, & Yi, 2016; Gibson, Birks, Yi, Moncur, & McEachern, 2016; Gonfiantini, 1986). Based on the Craig and Gordon (1965) resistance model, the isotopic composition of evaporation, as applied to evaporating lakes by Gibson, Birks, and Yi (2016), Gibson, Birks, Yi, Moncur, and McEachern (2016), and Gonfiantini (1986), can be estimated using:

$$\delta_E = \frac{1}{1 - h + 10^{-3}\Delta\varepsilon}\left(\frac{\delta_S - \varepsilon^{+}}{\alpha^{+}} - h\delta_A - 10^{-3}\Delta\varepsilon\right) \tag{3}$$

where h is humidity, δ_A is the isotopic composition (either $\delta^{18}O$ or $\delta^{2}H$, ‰) of the atmospheric moisture above the lake, δ_S is the steady-state isotopic composition (either $\delta^{18}O$ or $\delta^{2}H$, ‰) of the lake, α^{+} is the equilibrium fractionation factor, and ε^{+} and $\Delta\varepsilon$ are the equilibrium and kinetic enrichment factors, respectively (Craig & Gordon, 1965; Gibson, Birks, & Yi, 2016; Gibson, Birks, Yi, Moncur, & McEachern, 2016; Gonfiantini, 1986). The calculations in this study assume uniformity of environmental conditions above Bear Lake, implying that similar values apply across the lake surface. Substitution of Equation 3 into Equation 2 results in:

$$X = \frac{\delta_L - \delta_I}{A - \delta_L B} \tag{4}$$

where the terms A and B are given by (Gonfiantini, 1986):

$$A = \frac{h\delta_A + \Delta\varepsilon + \frac{\varepsilon^+}{\alpha^+}}{1 - h + 10^{-3}\Delta\varepsilon} \tag{5}$$

$$B = \frac{h - \Delta\varepsilon - \frac{\varepsilon^+}{\alpha^+}}{1 - h + 10^{-3}\Delta\varepsilon} \tag{6}$$

2.2. Isotopic Composition of Atmospheric Moisture and Enrichment Factors

Assuming equilibrium isotopic exchange between the precipitation (δ_P) and atmospheric moisture, the following equation, can be used to estimate the isotopic composition of the atmospheric moisture (δ_A):

$$\delta_A = \frac{(\delta_p - k\varepsilon^+)}{\left(1 + 10^{-3} \cdot k\varepsilon^+\right)} \tag{7}$$

where k is the constant accounting for seasonality in evaporation, ranging from 0.5 for highly seasonal climates to 1, representing non-seasonal climates (Gibson, Birks, & Yi, 2016; Gibson, Birks, Yi, Moncur, & McEachern, 2016). To give more weight to months with the highest lake isotopic enrichment due to evaporation, the average annual precipitation value is evaporation flux weighted. Given this, the k value for the calculations in this study is set to one. Accounting for seasonality is particularly important in climate settings where the lake surface freezes, suspending any isotope exchange due to evaporation (Gibson, Birks, & Yi, 2016; Gibson, Birks, Yi, Moncur, & McEachern, 2016). While the temperature goes below zero during the winter, the lake does not regularly freeze. Between 1995 and 2005, the lake remained unfrozen for 7 years (Dean et al., 2009).

The empirical equations for the equilibrium fractionation factor (α^+) for both isotopes are temperature-dependent and experimentally determined. Calculations in this paper are based on the equations derived by Horita and Wesolowski (1994), adopting the convention used by Gibson, Birks, and Yi (2016) and Gibson, Birks, Yi, Moncur, and McEachern (2016) where $\alpha^+ > 1$, representing the isotopic ratio in the liquid over the vapor:

$$\alpha^+\left({}^{18}O\right) = exp\left(\frac{-7.685}{10^3} + \frac{6.7123}{T} + \frac{1666.4}{T^2} + \frac{350410}{T^3}\right) \tag{8}$$

$$\alpha^+\left({}^{2}H\right) = exp\left(\frac{1158.8\ T^3}{10^{12}} - \frac{1620.1\ T^2}{10^9} + \frac{794.84\ T}{10^6} + \frac{-161.04}{10^3} + \frac{2999200}{T^3}\right) \tag{9}$$

where T is water temperature in Kelvin. The corresponding enrichment factor (ε^+) is equivalent to $1{,}000 \cdot (\alpha^+ - 1)$. Lastly, the kinetic enrichment factor ($\Delta\varepsilon$) for both isotopes are calculated using the following equation:

$$\Delta\varepsilon = \theta C_k \cdot (1 - h) \tag{10}$$

where θ is the transport resistance parameter, typically assigned the value of 1 when δ_A and humidity estimates relate to the air near the liquid interface (Gat, 1995). The kinetic constant, C_k, for lakes is commonly assigned the values of 14.2 and 12.5‰ for $\delta^{18}O$ and $\delta^{2}H$, respectively. These values were experimentally derived and are assumed to be the typical kinetic fractionation occurring in most evaporation processes in nature (Gibson, Birks, & Yi, 2016; Gibson, Birks, Yi, Moncur, & McEachern, 2016; Gonfiantini et al., 2020; Merlivat, 1978).

3. Data

3.1. Stable Isotope Data Set

The stable isotope data set used (Figure 1b) in this paper was compiled from the open-source, community database WaterIsotopes Database (WaterIsotopes Database, 2017; http://waterisotopes.org) and sampling campaigns conducted in May 2022 and August 2023, representing high runoff and dry seasons, respectively. The community

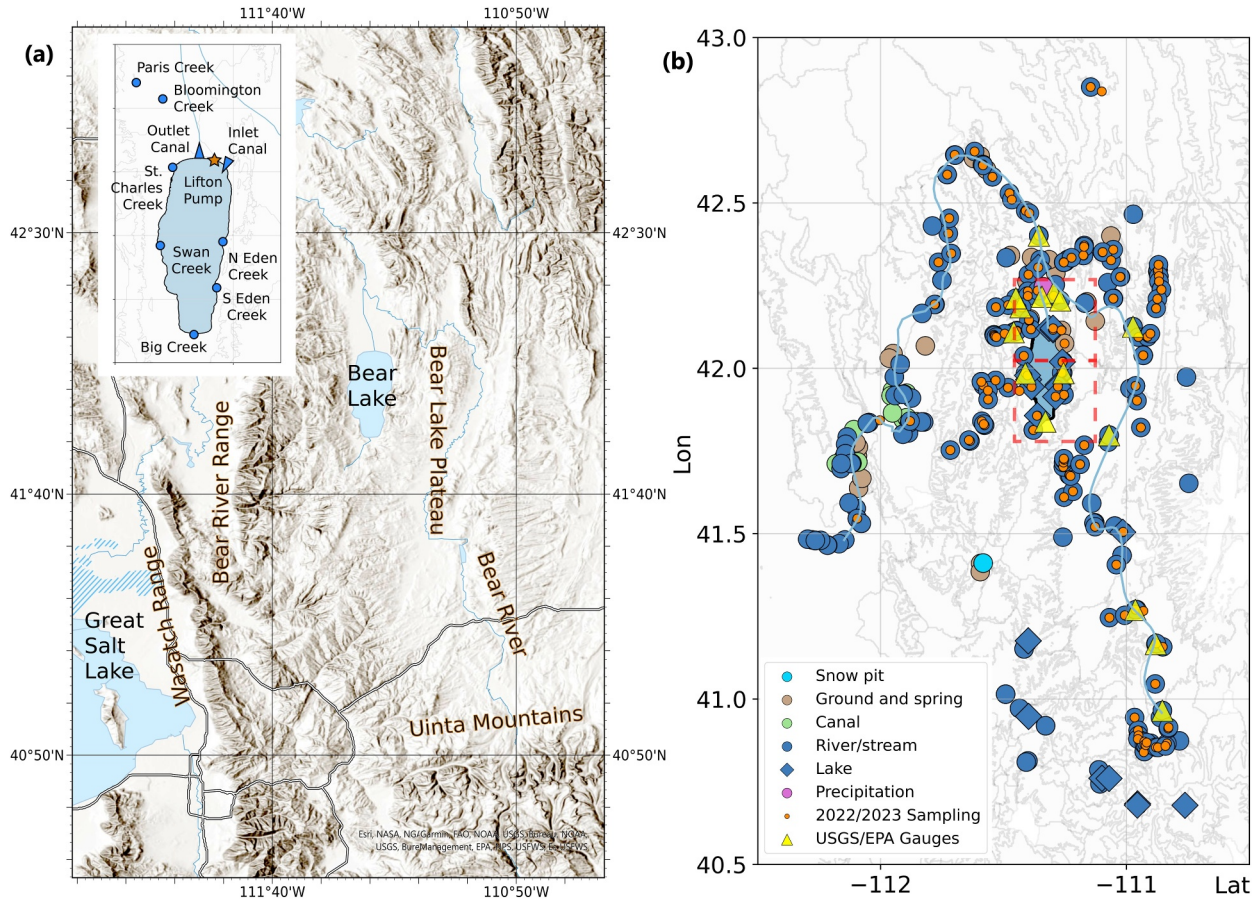

Figure 1. (a) Bear River watershed map (inset figure: location of surrounding creeks, inlet canal, Lifton pump station, and outlet canal). (b) Bear Lake study site and the compiled data set ($n = 688$; data used in the analysis: $n = 232$, excluding downstream Bear River and snow pit data). Breakdown of isotope data analyzed per hydrological component: Upstream Bear River ($n = 173$), Creek ($n = 19$), Precipitation ($n = 13$, 12 of which were based on OIPC estimates), Bear Lake ($n = 12$), Groundwater and Spring ($n = 18$), Downstream Bear River ($n = 103$), Snow pit data ($n = 3$, overlying a precipitation data point near 41.5° latitude), and Gauge stations used ($n = 14$). The orange dots refer to sampling sites visited during the 2022 and 2023 field campaigns. See Tables S2–S4 in Supporting Information S1 for more details. WaterIsotopes data come from https://wateriso.utah.edu/waterisotopes/pages/spatial_db/SPATIAL_DB.html (Brooks, 2014; Brooks et al., 2014; Fiorella, 2012; Friedman et al., 2002; Idaho Department of Water, 2015; Kendall, 1987; Utah Geological Survey, 2017; Yusuf, 2013). Red dashed boxes correspond to the NARR grids extracted.

database provided stream, precipitation, snow pit, lake, and groundwater data, while stream, spring, and lake water samples were collected from the field. The compilation spanned from October 1956 to August 2023 with discontinuous sampling intervals (Tables S3 and S4 in Supporting Information S1). Water samples obtained in May 2022 and August 2023 were analyzed at Vanderbilt University in Nashville, Tennessee, and Brown University in Providence, Rhode Island, using Picarro L2130-i and L2140-i cavity ring-down spectrometers, respectively. Available data for the isotopic composition of precipitation directly onto the lake surface was supplemented by estimates calculated from the Online Isotopes in Precipitation Calculator (OIPC), using the latitude, longitude, and average elevation of the lake surface as inputs (Bowen, 2017). The OIPC generates spatiotemporal data by interpolating existing isotope data, primarily from the Global Network of Isotopes in Precipitation (GNIP) data set (Bowen & Revenaugh, 2003; Bowen et al., 2005; IAEA/WMO, 2015; Welker, 2000).

3.2. Hydrological and Climate Data Sets

Monthly mean total evaporation at surface, precipitation amount, and humidity at surface data were extracted from the North American Region Reanalysis (NARR) data set produced by the NOAA National Center for Atmospheric Prediction (NCEP) (Mesinger et al., 2006). The NARR data set has a spatial resolution of 0.3° (~32 km) spanning from 1981 to 2010. The values utilized in this study came from the monthly long-term mean data set. A single value for each parameter was derived by taking the average of the two grid cells that encompass

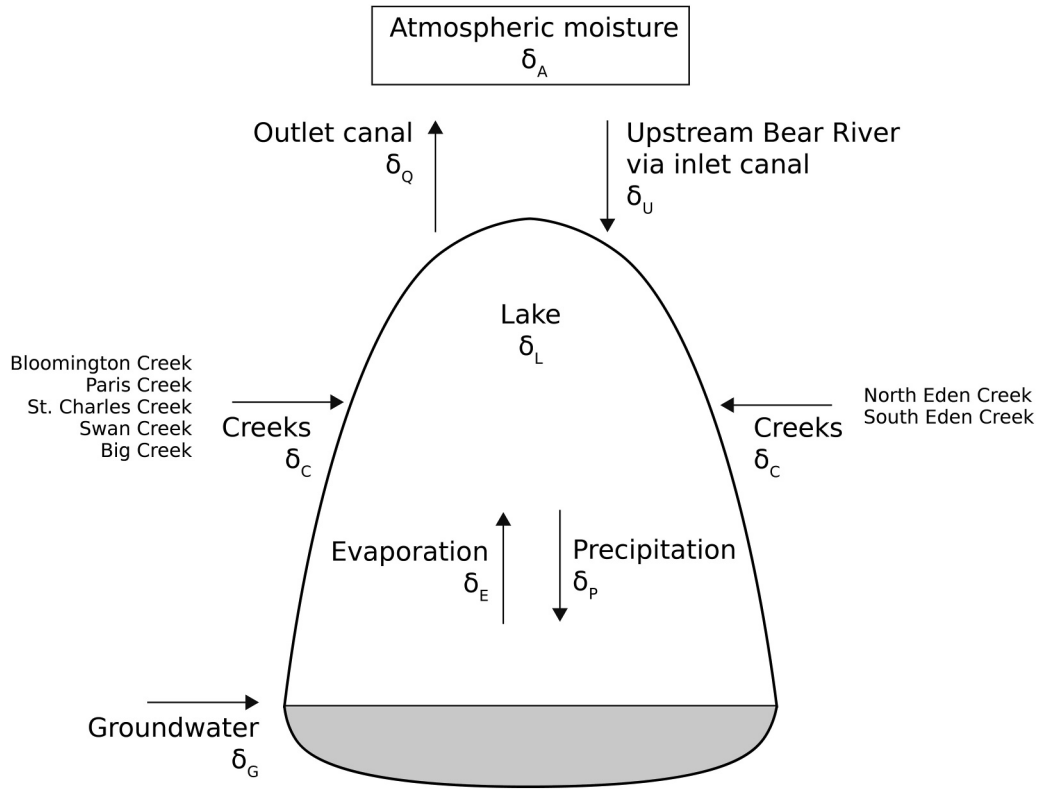

Figure 2. Major fluxes that maintain the volume of Bear Lake. Adapted from Bright (2009).

Bear Lake (red dashed boxes in Figure 1b). Temperature data was extracted from the National Weather Service (NWS) website based on a measuring station at the Lifton pump in Idaho (42.123, −111.3133). Discharge rates for the upstream Bear River and the surrounding creeks were acquired from a network of gauges maintained by the United States Geological Survey (USGS) and Utah Department of Environmental Quality obtained through the National Water Quality Monitoring Council Water Quality Portal (National Water Quality Monitoring Council, 2021; U.S. Geological Survey, 2024; https://www.waterqualitydata.us/).

4. Bear Lake Climate and Hydrology

A schematic diagram of the major hydrological fluxes that maintain the volume and isotopic composition of the lake is shown in Figure 2. Bear Lake is bounded by the Bear River Range in the west and the Bear Lake Plateau in the east. Most of the input volume comes from diverted water from the Bear River coursed through the Rainbow Inlet Canal. The headwaters of the Bear River stretch further south of the lake to the Uinta Mountains. Significant input also comes from springs and creeks that surround the lake, particularly those originating from the Bear River Range to the west. Several of these creeks are gauged, including Paris Creek, Bloomington Creek, St. Charles Creek, Swan Creek, and Big Creek, with average annual discharge rates ranging from 0.3 to 1.6 m^3/s. Discharge coming from the Bear Lake Plateau to the east is lower than that coming from the Bear River Range based on the monthly estimated discharge from the North Eden Creek, which ranges from 0.06 to 0.15 m^3/s (periodic data from 1942 to 2004; compiled by Bright, 2009). Most of the water that supplies streams surrounding the lake comes from instantaneous and delayed discharge of snowmelt from the surrounding mountains (Bright, 2009).

Similar to the rest of the western United States, climate in the region is modulated by atmospheric conditions over the North Pacific Ocean (Dean et al., 2009). The interaction of seasonal westerly winds coming from the Pacific and the Sierra Nevada and Cascade ranges leads to hot, dry summers and cold, wet winters in the study area (Dean et al., 2009). The lake receives most of its precipitation during the winter in the form of snow. Thus, peak stream and groundwater discharge inflow occurs during the melting of snow in spring. The limited moisture during summer is

Table 1
Mean Environmental Conditions and the Annual Influx of Each Input Component Based on Available Data

Parameter	Value	Calculation	Data source
Humidity/relative humidity, h	0.76[a]	Evaporation-flux weighted	NARR
Temperature, °C	11.15[a]	Evaporation-flux weighted	NWS
Temperature, °C	5.31	Mean	NWS
Upstream (through inlet canal) (f_U, m^3/yr)	3.18×10^8	Mean	USGS
Creeks (f_C, m^3/yr)	1.45×10^8	Mean	USGS and Utah DEQ
Precipitation (f_P, m^3/yr)	1.08×10^8	Mean	NARR
Outlet (f_Q, m^3/yr)	3.53×10^8	Mean	USGS

[a]The humidity and temperature values, derived from the reported data of the cited sources, serve as the initial inputs for the calculations described in Section 5.2.1.

brought by monsoon rains originating from the Gulf of Mexico and Gulf of California (Bright, 2009; Dean et al., 2007, 2009).

Routine operations of the Lifton pump at Bear Lake are designed to respond to seasonal hydrology (star in Figure 1a inset). In spring, the pump diverts upstream river runoff into the lake for storage, except in cases when the lake reaches capacity later in the season, prompting the diversion of excess water downstream into the Bear River. During the summer, when evaporation rates are high, stored water is pumped out of the lake. Additional controls, particularly during the fall and winter seasons, depend on irrigation or flood management needs (PacifiCorp, 2019). Table 1 summarizes the mean annual data from available climate and hydrologic data sets described in Section 3.2, while Figure 3 shows a plot of monthly averages (1981–2010 for climate data sets; 1942–2023 for hydrologic data sets) of the same parameters. Seasonal volume-weighted calculations are arbitrarily based on the monthly hydrological plots, assigning March to July as the wet season and the rest of the months as dry season. Measured groundwater discharge records are unavailable, but comparisons between lake

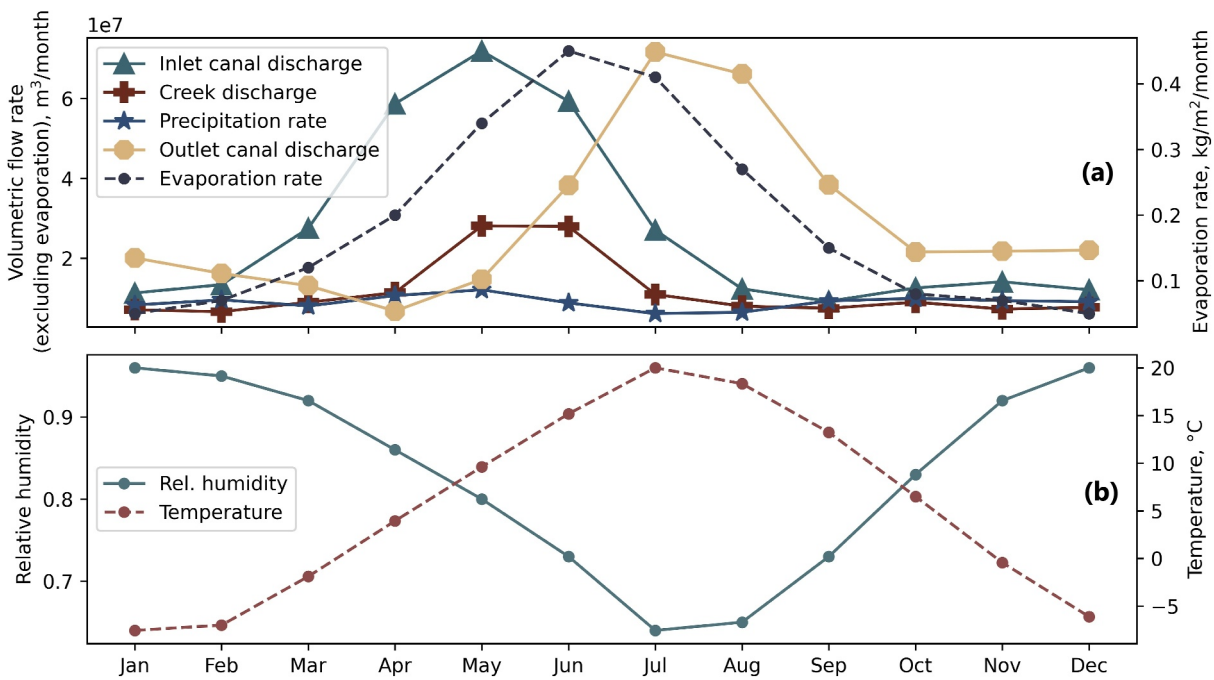

Figure 3. (a) Climatological monthly evaporation and precipitation rates derived from the NARR data set (1981–2010) and discharge means of the inlet and outlet canals and the surrounding creeks (1942–2023). (b) Climatological monthly means of humidity derived from the NARR data set (1981–2010) and surface water temperature (2000–2024). Evaporation, precipitation, and humidity data encompass the Bear Lake and surrounding land area within the NARR grid cells extracted.

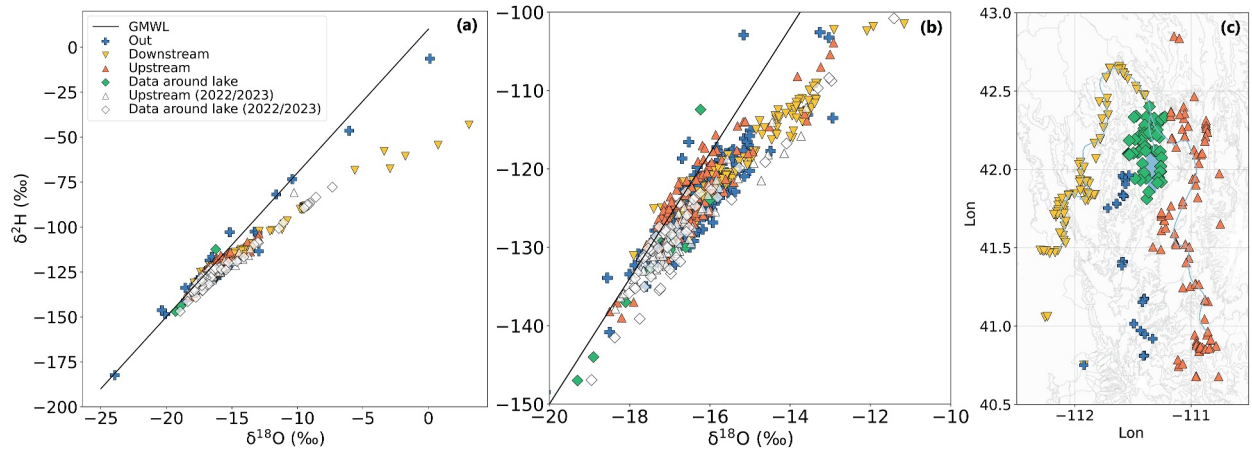

Figure 4. (a) Bear River watershed isotopic data set and the Global Meteoric Water Line (GMWL). (b) Zoomed figure of panel (a). The white markers for upstream and around lake data represent values from the May 2022 and August 2023 field campaigns. (c) Reference map of data points grouped spatially.

level and water table data suggest recharge from groundwater (Table S1 in Supporting Information S1). An estimate of groundwater discharge is calculated in Section 5.2.2.

5. Results

5.1. Watershed Stable Isotope Data

Figure 4 is a plot of the spatial subgroups of the isotope data set relative to the Global Meteoric Water Line (GMWL). Evaporative enrichment is evident in several of the meteoric water samples around the lake and downstream in the Bear River as shown by the deviation of these points from the GMWL. A number of these data points are samples from Bear Lake and the Great Salt Lake where the Bear River drains.

Table 2 provides a summary of the isotopic composition of the identified components of the total inflow (Figure 2). These values are derived from all the data under the "Upstream" and "Data around lake" subgroups (Figure 4) and use the monthly evaporation data (Figure 3) to get the evaporation flux-weighted values. The average isotopic composition of the waters from upstream Bear River, surrounding creeks, and groundwater exhibit relatively minor variations, suggesting similarly depleted sources compared to precipitation. This source water likely originates from the snowmelt-influenced headwaters situated within the Bear River Range and Uinta Mountains. Available snow pit isotope data from the WaterIsotopes community database indicate mean values of −21.46 and −159.08‰ for $\delta^{18}O$ and $\delta^{2}H$, respectively (Utah Geological Survey, 2017).

5.2. Mass Balance Calculations

The isotopic mass balance calculations were done in two phases. First, we implement Equation 4 separately for $\delta^{18}O$ and $\delta^{2}H$. Afterward, a system of nonlinear equations was set up to simultaneously solve for multiple unknowns (groundwater discharge, f_G; evaporation flux, E; evaporation/inflow, X; isotopic composition of total inflow, δ_I ^{18}O and δ_I ^{2}H; and humidity, h; see Table 4).

5.2.1. Separate Mass Balance Calculations for Both $\delta^{18}O$ and $\delta^{2}H$

Preliminary iterations determining the evaporation/inflow (X in Equation 4) involved separate sets of calculations for each isotope. Assuming insignificant contribution, groundwater influx as part of the total volume input was ignored for this first set of calculations. Table 3 summarizes the input and output values for the individual mass balance calculations.

The evaporation/inflow terms (X) derived from each isotope differ by 0.13. Further evaluation of the outputs reveals inconsistencies in the mass balance when the measured lake isotopic data is compared to the anticipated trend of isotopic enrichment (Figure 5a) with the given input climate (Table 1) and isotopic data (Table 2). With

Table 2
Mean Annual Influx Data of the Input Components

Parameter	Variable	Value	n	Standard deviation	Calculation
Upstream Bear River (via inlet canal), ‰	δ_U ^{18}O	−16.57	173	1.08	Volume and seasonal inlet discharge-weighted
Upstream Bear River (via inlet canal), ‰	δ_U ^{2}H	−125.87	172	6.87	Volume and seasonal inlet discharge-weighted
Creeks, ‰	δ_C ^{18}O	−16.64	19	0.96	Volume and seasonal creek discharge-weighted
Creeks, ‰	δ_C ^{2}H	−126.20	19	5.95	Volume and seasonal creek discharge-weighted
Precipitation[a], ‰	δ_P ^{18}O	−14.60	13	4.83	Monthly volume-weighted
Precipitation[a], ‰	δ_P ^{2}H	−105.70	13	36.87	Monthly volume-weighted
Precipitation[a], ‰	δ_P ^{18}O	−11.70	13	4.83	Monthly evaporation flux-weighted
Precipitation[a], ‰	δ_P ^{2}H	−84.02	13	36.87	Monthly evaporation flux-weighted
Groundwater, ‰	δ_G ^{18}O	−17.80	18	0.78	Mean
Groundwater, ‰	δ_G ^{2}H	−135.74	18	6.22	Mean
Lake, ‰	δ_L ^{18}O	−8.76	12	0.73	Mean
Lake, ‰	δ_L ^{2}H	−86.44	9	3.42	Mean

[a]Volume-weighted value is used for inflow calculations; evaporation flux-weighted value is used for estimating δ_A. Data histograms for each component can be found in Figure S1 in Supporting Information S1.

groundwater excluded from the calculations, Figure 5 shows the current lake data plotted against the theoretical trend of the lake water δ^2H-$\delta^{18}O$ composition during evaporation under conditions of varying relative humidity.

The slope of the current measured Bear Lake water isotopic composition and the calculated maximum enrichment it can reach deviates from the theoretical evaporation trend at the input humidity of 0.76 (Figure 5). The theoretical maximum is calculated by dividing the terms *A* and *B* from Equations 5 and 6 (Gibson, Birks, & Yi, 2016; Gibson, Birks, Yi, Moncur, & McEachern, 2016; Gonfiantini, 1986). Assuming an *X* value of 0.435, which is the average of the previously calculated values for $\delta^{18}O$ and δ^2H, the isotopic composition of the lake based on the

Table 3
Initial Inputs and Outputs to the Model

Parameter	^{18}O	^{2}H	Calculation
Fractionation and enrichment factors			
Equilibrium fractionation factor (a^+, ‰)[a]	1.011	1.095	Equations 8 and 9
Equilibrium enrichment factor (ε^+, ‰)	10.61	95.42	$1{,}000\cdot(a^+ - 1)$
Kinetic enrichment factor ($\Delta\varepsilon$, ‰)[a]	3.41	3.00	Equation 10
Input values			
Total volume input (δ_I, ‰)[b]	−16.22	122.14	Discharge-weighted
Atmospheric moisture (δ_A, ‰)	−22.08	−163.8	Equation 7
Output values			
Evaporation/Inflow (X)	0.50	0.37	Equation 4
Evaporation rate, m^3/yr	2.83×10^8	2.11×10^8	
Evaporate (δ_E, ‰)	−23.82	−183.2	Equation 3

[a]Based on available data on annual evaporation flux-weighted humidity = 0.76 and temperature = 11.15°C. [b]Using available isotopic and discharge data. The rest of the parameters were calculated using the indicated equation.

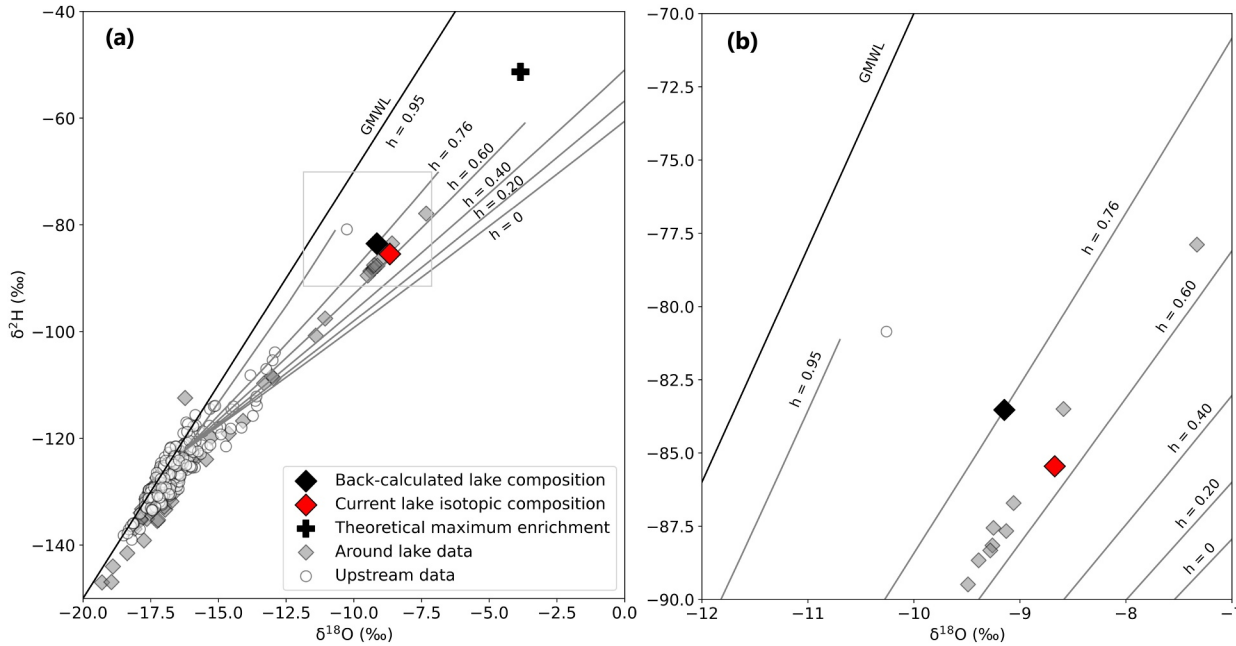

Figure 5. (a) Current isotopic composition of Bear Lake plotted against theoretical evaporation lines at different humidity levels. (b) Zoomed figure of boxed area in panel (a).

input humidity and temperature should theoretically be −9.15 and −83.53‰ for $\delta^{18}O$ and $\delta^{2}H$, respectively (black diamond in Figure 5).

Most of the difference between the back-calculated (black diamond in Figure 5) and current (red diamond in Figure 5) isotopic composition of the lake comes from $\delta^{18}O$, with the back-calculated value being isotopically lighter by about 0.39‰. While taking the standard deviation of the available raw lake values into account will reduce this discrepancy (Table 2), it is also important to note that all raw lake values deviate from the $h = 0.76$ line (gray diamonds in Figure 5). This discrepancy underscores the greater sensitivity of the oxygen isotope ratio to kinetic transport compared to $\delta^{2}H$ (cf. Gonfiantini, 1986), as evidenced by the substantial contribution of the calculated kinetic enrichment factor for $\delta^{18}O$ to its total enrichment factor (Table 3). Humidity primarily dictates the magnitude of kinetic transport; hence, it significantly contributes to uncertainties in isotope mass balance calculations in semi-arid environments such as Bear Lake (Gibson, Birks, & Yi, 2016; Gibson, Birks, Yi, Moncur, & McEachern, 2016). This is reflected in the changes in the theoretical evaporation slope with humidity (Figure 5).

Additionally, uncertainties on input isotopic and climate data can contribute to this discrepancy. As discussed in later sections, capturing the influence of seasonality in evaporation is crucial to accurately represent annually integrated isotopic processes. Given the differences observed in the individual mass balance calculations, we move on to solve a system of equations using both isotope systems.

5.2.2. Constraining the Hydrological Balance Using a System of Equations

In order to obtain a single solution for the evaporation/inflow (X) incorporating both $\delta^{18}O$ and $\delta^{2}H$ data, the next step of the calculations involved setting up a system of equations using the mass balance formula for both isotopes. Introducing groundwater discharge (f_G) as an unknown input renders the isotopic composition of the total volumetric input to the lake as an unknown (δ_I), which is calculated for each isotope via discharge-weighted averaging (See Tables 1 and 2 for the components represented by each variable):

$$\delta_I = \frac{\delta_I \cdot f_I + \delta_C \cdot f_C + \delta_P \cdot f_P + \delta_G \cdot f_G}{f_I + f_C + f_P + f_G} \tag{11}$$

Table 4
Solutions for the Unknown Parameters and the Relevant Equations Used

Unknown parameters	Variable	Relevant equations	Solved value
Groundwater discharge, m^3/yr	f_G	Equation 1, where $I = f_G + f_U + f_C + f_P$, $Q = f_U$, and E is evaporation	7.62×10^4
Evaporation flux, m^3/yr	E	Equation 2	2.18×10^8
Evaporation/Inflow	X	Equation 4, applied separately to $\delta^{18}O$ and δ^2H	0.38
$\delta^{18}O$ of total inflow, ‰	$\delta_I\ ^{18}O$	Equation 11	−16.22
δ^2H of total inflow, ‰	$\delta_I\ ^{2}H$	Equation 11	−122.2
Humidity	h	Equation 4, where $\Delta\varepsilon$ is calculated using Equation 10	0.62

Assuming that the lake is hydrologically balanced (Equation 1) and all other major fluxes are identified and calculated (Figure 2), groundwater discharge should be represented by the residual after accounting for the volumetric inflows with known values (upstream Bear River, creeks, and precipitation) and outflows (outlet canal and evaporation). The final evaporation volume flux (E) can then be calculated using Equation 2.

For this calculation, the measured isotopic compositions and volumetric flow rates of the lake, known components of the inflows, and known components of the outflows are maintained as constant (Tables 1 and 2). Additionally, the isotopic composition of the water exiting through the outlet canal is assumed to be equal to the lake itself, while the isotopic composition of atmospheric moisture is taken from Table 3. Similar to Section 5.2.1, temperature is set to 11.15°C. Therefore, the same equilibrium fractionation and enrichment factors were used (Table 3).

In summary, a system of six nonlinear equations was constructed to solve for six unknowns. The Powell hybrid method, which is implemented in the Python function *fsolve* included in the standard SciPy package, was used to solve for the roots (Powell, 1970; Virtanen et al., 2020). Table 4 summarizes all the unknown variables and the derived solutions.

Humidity was also treated as an unknown with a calculated value of $h = 0.62$, lower than the value extracted from the NARR data set ($h = 0.76$). In the Craig-Gordon model, the relevant humidity value is the boundary between the turbulent region and free air, implying that it is the humidity right above the lake that modulates the evaporation process. In practice, this can be difficult to measure (i.e., rarely measured directly), as humidity is usually taken meters above the lake surface or at nearby weather stations not adjacent to the lake shoreline. The NARR-derived humidity value, as a reanalysis product, is an interpolation of nearby humidity values not necessarily within Bear Lake. In addition, wind direction induces spatial variations in the distribution of atmospheric moisture (Craig & Gordon, 1965; Gonfiantini, 1986; Gonfiantini et al., 2020). These uncertainties can account for the discrepancy between the theoretical and observed data.

5.3. Uncertainty Calculations and Sensitivity Tests

Table 5 summarizes all values for the environmental conditions and isotopic components of the Bear Lake mass balance system derived from the calculations performed in the preceding sections. Uncertainty estimates listed for the input variables are either estimated or adapted from the reported typical measurement accuracies for each specific parameter (Picarro, 2024).

The combined uncertainty for X (Evaporation/Inflow) is determined by running Monte Carlo calculations separately for $\delta^{18}O$ and δ^2H mass balance equations. Random input values with uniform distributions were generated based on the error estimates listed in Table 5 for each parameter. The combined uncertainty is taken to be a unit of standard deviation from an ensemble of 100,000 simulations. Generally, using $\delta^{18}O$ data gave a slightly higher uncertainty than δ^2H-based estimates for both the X and E terms (Table 5).

Sensitivity analysis of X to the input parameters was conducted for both $\delta^{18}O$ and δ^2H using the Sobol method as implemented in the Python package *SAlib* (Herman & Usher, 2017; Iwanaga et al., 2022). Figure 6 summarizes the calculated normalized first-order (S1) Sobol index, which measures the first order sensitivity of the output to each individual input parameter.

Table 5
Summary of the Calculated Components of the Isotopic Mass Balance at Bear Lake

Parameter	Variable	Value	Estimated error	Source of error value
Environmental conditions				
Evaporation season humidity	h	0.62	0.031 (5%)	Estimated
Evaporation flux-weighted temperature (°C)	T	11.15	0.2	U.S. Geological Survey (2008)
Solved evaporation data				
Evaporation flux, m^3/yr	E	2.18×10^8	4.94×10^6 using $\delta^{18}O$, 3.47×10^6 using δ^2H	Uncertainty calculations, 1σ
Evaporation/Inflow	X	0.382	0.009 using $\delta^{18}O$, 0.006 using δ^2H	Uncertainty calculations, 1σ
Evaporate, ‰	$\delta_E\ ^{18}O$	−28.22	0.55	Uncertainty calculations, 1σ
Evaporate, ‰	$\delta_E\ ^{2}H$	−179.88	4.35	Uncertainty calculations, 1σ
Input isotopic data				
$\delta^{18}O$ of total inflow, ‰	$\delta_I\ ^{18}O$	−16.22	0.05	Calculated combined uncertainty
δ^2H of total inflow, ‰	$\delta_I\ ^{2}H$	−122.15	0.24	Calculated combined uncertainty
Evaporation flux-weighted precipitation, ‰	$\delta_P\ ^{18}O$	−11.70	0.04 (0.3%)	Bowen (2017), Bowen and Revenaugh (2003)
Evaporation flux-weighted precipitation, ‰	$\delta_P\ ^{2}H$	−84.02	0.84 (1%)	Bowen (2017), Bowen and Revenaugh (2003)
Atmospheric moisture, ‰	$\delta_A\ ^{18}O$	−22.08	0.02	Based on evaporation-flux weighted precipitation
Atmospheric moisture, ‰	$\delta_A\ ^{2}H$	−163.81	0.46	Based on evaporation-flux weighted precipitation
Lake, ‰	$\delta_L\ ^{18}O$	−8.76	0.1	Estimated
Lake, ‰	$\delta_L\ ^{2}H$	−86.44	0.5	Estimated

Note. All values correspond to annual means.

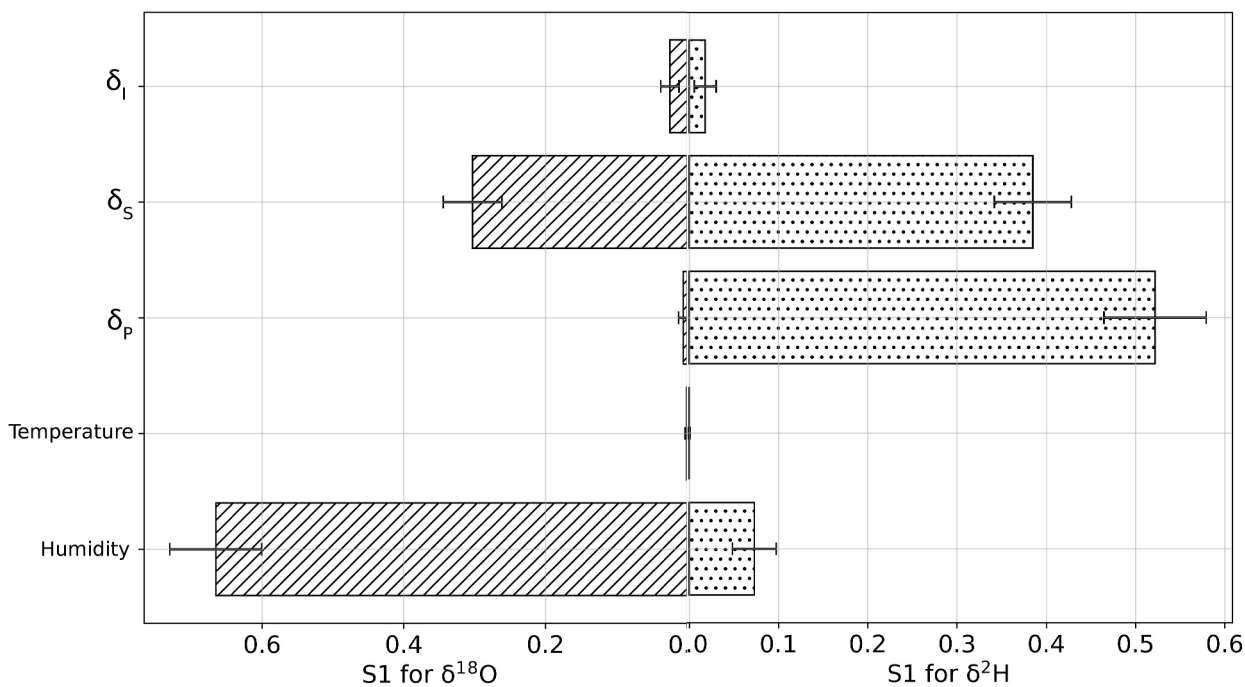

Figure 6. Calculated Sobol first-order index (S1) to measure the response of *X* (Evaporation/Inflow) to humidity, temperature, and the isotopic compositions of the evaporation flux-weighted precipitation (δ_P), steady-state lake (δ_S), and total inflow (δ_I). Left bars correspond to $\delta^{18}O$ mass balance, right bars correspond to δ^2H mass balance. The complete table of calculated Sobol indices, which includes the second-order index (S2) and total index (ST) can be found in the supplementary materials (Table S6 in Supporting Information S1).

The S1 term corresponds to the relative first order response of X to the input parameters. The sum of the values assigned to each parameter is one. Based on the values calculated, $\delta^{18}O$-derived X appears to be the most sensitive to humidity and δ_S, while δ^2H-derived X is most sensitive to evaporation-flux weighted (δ_P), steady-state lake isotopic composition (δ_S), and humidity. Meanwhile, the second-order index (S2) parameter measures the degree of interaction between pairs of parameters. The calculated S2 values for each pair of input parameters are all near zero (Table S6 in Supporting Information S1), suggesting negligible cross-interactions between variables. This implies each parameter exerts independent influence on lake evaporation rates. Interestingly, $\delta^{18}O$-based calculations are most sensitive to humidity uncertainties, while δ^2H-based values are more sensitive to the evaporation-flux weighted δ_P variations. This further highlights the greater sensitivity of $\delta^{18}O$ to kinetic fractionation processes relative to δ^2H. Meanwhile δ^2H appears to respond more to the gradient of isotopic composition in the air, as the evaporation flux-weighted δ_P is used to estimate δ_A.

Given these results, individual sensitivity tests were performed on the $\delta^{18}O$ and δ^2H-derived evaporation rates to changes in humidity and δ_A. Overall, X increases with decreasing humidity and isotopically lighter atmospheric moisture for both $\delta^{18}O$ and δ^2H. A sharper change in X occurs when humidity reaches around 0.30 to 0.35 for $\delta^{18}O$ and δ^2H-based calculations, while the generated slopes for X versus δ_A are comparable for each isotope, with $\delta^{18}O$ being steeper (slope/mean output: -1.38 for $\delta^{18}O$ and -0.86 for δ^2H, Figure S2 in Supporting Information S1). While both parameters are critical inputs, the Sobol sensitivity analysis suggests that humidity has more influence on $\delta^{18}O$-based evaporation rates (Figure 6).

6. Discussion

6.1. Isotopic and Hydrologic Mass Balance of the Lake

The calculations performed in the preceding sections demonstrate the utility of water isotopes in constraining hydrological fluxes, particularly evaporation, within lake systems. Converting the calculated evaporation rate (2.18×10^8 m^3/yr, Table 5) and comparing it to several approximations found in the literature, we find that our estimate (2.10 mm/day, when converted to length per time) is consistent with available annual data: ~2.7 mm/day (Kaliser, 1972) and 2 mm/day (Amayreh, 1995). It must be noted that the referenced values were obtained through evaporation pan methods at limited sampling intervals and may not be representative of the annual daily average (Amayreh, 1995; Kaliser, 1972). Using a lake volume of 7.89 km^3 (based on the physical-morphometric characteristics of the lake, Lamarra et al., 1986) and the balanced total input/output volumetric fluxes (0.57 km^3/yr, converted from Tables 1 and 4), the water residence time at Bear Lake is approximately 13.8 years. The isotopic composition of the lake reflects the integrated influence of hydrological processes over the residence period of the water within the lake. Therefore, the evaporation rates calculated in this study represent the long-term mean lake conditions over the approximated residence time (Gat, 1995).

The simultaneous estimation of evaporation rates and groundwater discharge using the iterative method in Section 5.2.2 assumes hydrological mass balance with a residual of zero. Previous work using geochemical and physical data has demonstrated that the modern Bear Lake is hydrologically balanced, or nearly so (Bright, 2009; Bright et al., 2006; Lamarra et al., 1986). The estimated groundwater discharge into the lake (7.62×10^4 m^3/yr, Table 4) shows that there is substantial inflow; however, it is orders of magnitude lower than the inflow from the other components of the lake balance (Table 1). Groundwater being slightly isotopically lighter than Bear River and the surrounding streams (Table 2) may represent the absence of evaporative enrichment similar to surface waters or suggest extrabasinal sources which can flow through faults and fractures (Bright, 2009). While it appears that groundwater has a minor influence on modern lake isotopic composition, it might be a more important component during past periods where the lake is disconnected from the Bear River (Bright et al., 2006; Kaufman et al., 2009). Additional isotopic data from groundwater and the vertical profile of the lake could help better constrain groundwater flow rates and lake mixing.

Figure 7 plots the estimated isotopic compositions of the evaporate (δ_E) and atmospheric moisture (δ_A) against lake and evaporation flux-weighted precipitation data. The blue dashed line represents the evolution of evaporation in the lake. The calculated slope ($m = 4.80$) lies within the typical range (4–5) for temperate lakes, which is the intermediate response between high and low-latitude open waters (Gibson, Birks, & Yi, 2016; Gibson, Birks, Yi, Moncur, & McEachern, 2016). However, it should be noted that the isotopic compositions of the inflow and precipitation are different, with the inflow considerably lighter than precipitation. This difference likely reflects

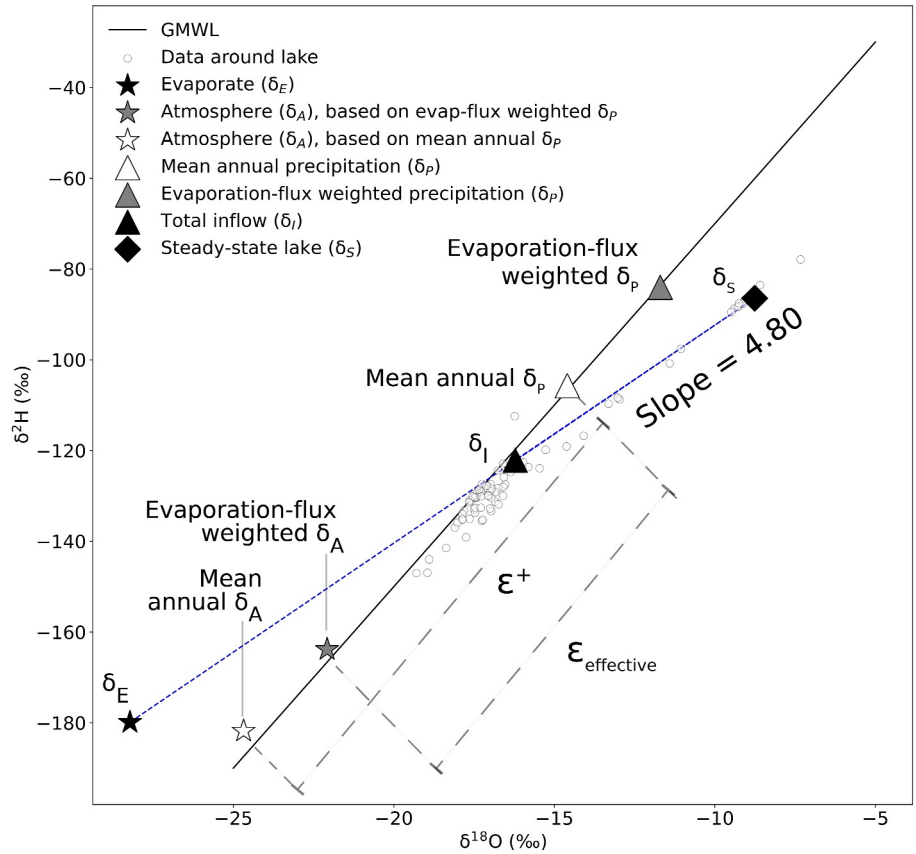

Figure 7. Schematic $\delta^{18}O$-$\delta^{2}H$ plot showing the isotopic composition of water in the different components of the lake balance. Shown are data for the evaporate, atmospheric moisture, precipitation, total inflow, and lake.

the input of isotopically depleted snowmelt coming from high elevation areas in the Uinta Mountains. Other sources of inflow water come from runoff from the Bear River Range, which feeds the creeks on the western side of the lake (Bright, 2009; Dean et al., 2009).

The separation of the mean annual (volume-weighted) δ_P from the δ_A based on evaporation-flux weighted δ_P, designated as $\varepsilon_{effective}$ in Figure 7, is approximately 76% of its separation from the δ_A derived from the mean annual δ_P, which estimates equilibrium enrichment (ε^+) at Bear Lake without accounting for any seasonality. This calculated difference aligns with the review of Gibson, Birks, and Yi (2016) and Gibson, Birks, Yi, Moncur, and McEachern (2016) where on average, the $\varepsilon_{effective}$ of temperate lakes is 75% of the ε^+. This difference between the $\varepsilon_{effective}$ and ε^+ reflects the influence of the seasonality of evaporation flux which will not be captured if only the mean annual (volume-weighted) data is used. Hence, temperature, precipitation, and atmospheric moisture during the evaporation season are better at estimating annual evaporation rates. This applies to Bear Lake due to the highly seasonal nature of evaporation and precipitation in the area (Figure 3).

6.2. Limitations

As demonstrated by the sensitivity analysis conducted (Figure 6), aside from the lake composition itself, humidity and δ_A regulate the rate and isotopic composition of evaporating water from Bear Lake. This finding has been pointed out in previous lake balance studies (Gibson, Birks, & Yi, 2016; Gibson, Birks, Yi, Moncur, & McEachern, 2016; Gibson et al., 2008; Gonfiantini, 1986; Gonfiantini et al., 2020). However, the sensitivity calculations performed in this study show that the relative importance of humidity and δ_A on the evaporation estimates is based on the water isotope used, with the former relatively more important in $\delta^{18}O$-based calculations, while the latter is more important in $\delta^{2}H$-based calculations. Hence, depending on the isotope system used,

constraining the accuracy of these two parameters should be emphasized to obtain better evaporation rate estimates.

An important assumption made in the calculations is the uniformity of environmental conditions across Bear Lake. As described by the Craig-Gordon model, fractionation during the evaporation process is dictated by the different layers above an open water body that modulate kinetic and equilibrium processes. The literature has been consistent with constraining the equilibrium fractionation process. However, the kinetic aspect is yet to be well-constrained, hence, much of the uncertainty stems from humidity and δ_A (Gonfiantini et al., 2020; Pierchala et al., 2022; Zannoni et al., 2022). Another important factor is wind, which can be accounted for by factoring in turbulence (n) into Equation 10 (Pierchala et al., 2022). The value of n can vary from zero (pure turbulent transport) to one (pure moleculer diffusion). Wind speed and direction can influence the distribution of moisture across the lake, impacting evaporation rate homogeneity (Horita et al., 2008; Pierchala et al., 2022; Zannoni et al., 2022). Additionally, wind can dismantle the laminar layer above the lake, as demonstrated experimentally by Gonfiantini et al. (2020) using pan evaporation methods. Additional wind turbulence decreases the kinetic isotopic fractionation by allowing the transport of vapor generated from equilibrium evaporation directly to turbulent atmosphere without additional fractionation (Brutsaert, 1975; Gonfiantini et al., 2020; Pierchala et al., 2022).

However, the natural wind structure above a lake is different from the artificial winds generated in a controlled evaporation pan setup. While the winds above Bear Lake (3–4 m/s, Table S5 in Supporting Information S1) exceed the ∼2 m/s threshold defined by Gonfiantini et al. (2020) up to which the Craig-Gordon model holds, scaling this result to a lake may not be applicable. To better examine wind effect, site-specific measurements, especially those capturing fetch-dependent isotopic fractionation, should be acquired to better quantify wind influence on the lake's evaporation dynamics.

6.3. Climate Scenarios

In this section, we explore changes in lake evaporation through time by simulating the climate conditions during the last interglacial period (LIG, ∼126 to 119 kyr ago), last glacial period (LGP, ∼115 to 11.7 kyr ago), and future warming events due to anthropogenic emissions. Available $\delta^{18}O$ carbonate records from Bear Lake sediment cores that are assumed to correspond to marine oxygen-isotope stage (MIS) 5e for the LIG and MIS 2 to 4 for the LGP, were used to estimate past lake isotopic composition (Bright et al., 2006; Kaufman et al., 2009). For the future warming scenario, we used the conditions during the LIG period, specifically the temperature and humidity, as a probable analog for anthropogenic climate change within the 21st century, assuming continued greenhouse gas emissions. While the forcing mechanisms for warming are different between the two scenarios (changes in insolation compared to increased CO_2 emissions), the warm conditions and comparable sea levels during the LIG have been used as a reference point for predictive climate models (Braconnot et al., 2012; Felis et al., 2015; Lunt et al., 2013).

Previous studies have suggested warmer (∼1°C higher) and drier conditions during MIS 5e globally, including North America, compared to the present (Berger, 1978; de Wet et al., 2023; Dutton & Lambeck, 2012; Kukla et al., 2002; Shackleton et al., 2020; Suh et al., 2020). Correspondingly, bulk lake sediment samples formed during MIS 5e recorded isotopically enriched (mean $\delta^{18}O$: −5.6 ± 1.9‰ VPDB) carbonates relative to the succeeding and preceding time periods (mean MIS 5a-d $\delta^{18}O$: −9.8 ± 1.9‰ VPDB; mean MIS 6 $\delta^{18}O$: −9.5 ± 0.9‰ VPDB), further supporting the inferred evaporative conditions (Kaufman et al., 2009). As a result of the warmer and drier conditions, the lake is suggested to be topographically closed and hydrologically disconnected from the Bear River during the LIG (Bright et al., 2006; Kaufman et al., 2009).

Meanwhile, MIS 2 to 4 are thought to be drier and cooler globally on average than the present, particularly during the last glacial maximum (LGM, ∼4–7°C lower) (Bush & Philander, 1999; Tierney et al., 2020). The average $\delta^{18}O$ of the bulk lake sediments that correspond to this period is −9.5 ± 0.9‰ VPDB. This relatively lighter isotopic composition is assumed to be due to instances of hydrological connections between the lake and the isotopically lighter Bear River. Surficial deposits north of the lake are thought to approximate the maximum extent of the Bear Lake shoreline around 40 kyr ago (11 m above modern lake level). The extended lake shoreline facilitated the then-connection between the lake and a segment of the Bear River, allowing the influx of snowmelt-derived river water (Bright et al., 2006; Kaufman et al., 2009; Laabs & Kaufman, 2003). Evidence of

Table 6
Assumed Input Conditions Required to Quantify Evaporation During LIG, LGP, Current, and Future Climate Scenarios

Parameter	LIG	LGP	Current[a]	Future	Distribution
Assumed environmental conditions relative to current	Warmer and drier	Colder	–	Warmer and drier	–
Connected to Bear River?	No	Yes	Yes	Yes	–
Lake $\delta^{18}O$, ‰ VSMOW	-7.2 ± 2.0[b]	-13.13 ± 0.9[b]	-8.76 ± 1.0	-8.76 ± 1.0	Uniform
Temperature (evaporation season), °C	$12.15 \pm 4\sigma$[c], $\sigma = 0.3$	$5.15 \pm 4\sigma$[c], $\sigma = 0.3$	$11.15 \pm 4\sigma$, $\sigma = 0.3$	$12.15 \pm 4\sigma$[c], $\sigma = 0.3$	Normal
Humidity (evaporation season)	$0.52 \pm 4\sigma$[d], $\sigma = 0.03$	$0.52 \pm 4\sigma$[d], $\sigma = 0.03$	$0.62 \pm 4\sigma$, $\sigma = 0.03$	$0.52 \pm 4\sigma$[d], $\sigma = 0.03$	Normal
Inflow $\delta^{18}O$, ‰	-15.77[e]	-16.22	-16.22	-16.22	–
Evaporation-flux weighted precipitation $\delta^{18}O$, ‰	-11.7	-11.7	-11.7	-11.7	–
X[f] (Evaporation/Inflow)	0.45 ± 0.1	0.12 ± 0.02	0.38 ± 0.05	0.36 ± 0.04	–

[a]Uncertainties for the input parameters representing the current scenario were widened to match other scenarios. [b]Converted from the $\delta^{18}O$ value of lake sediment carbonates (Bright et al., 2006; Kaufman et al., 2009) using empirical equations from O'Neil et al. (1969) and Coplen et al. (1983). The carbonate values are assumed to be authigenic. Mean annual lake temperatures of 6.31°C (+1°C from current, Table 1) and −0.69°C (−6°C from current) for the LIG and LGP, respectively, were assumed. However, it must be noted that lake water does not change in temperature at the same rate as air (Terrazas et al., 2023). [c]Scenarios that are assumed to be warmer than current: +1°C; and colder than current (LGP): −6°C. [d]All other scenarios are assumed to be drier than the current (−0.1 humidity). [e]Volume-weighted average of input components, excluding upstream Bear River (Table 2). It is assumed that the lake is hydrologically disconnected from the river during the LIG. [f]Uncertainties were derived from the one standard deviation spread of the generated data set (15.9th and 84.1st percentile).

glaciation in the Bear River watershed is found from sediments in the lake and the headwaters of Bear River in the Uinta Mountains (Laabs et al., 2007; Rosenbaum et al., 2012).

Following the conditions described for the different scenarios, Table 6 summarizes the assumed values of the input parameters to the isotopic mass balance model and the calculated *X*. A similar Monte Carlo simulation approach ($n = 100{,}000$) as performed in Section 5.3 was adopted to generate a spectrum of *X* values based on assumed distributions of lake $\delta^{18}O$, humidity, and temperature.

Expectedly, the LIG and LGP periods yielded significantly higher and lower *X* terms when compared to current *X* (0.382 ± 0.009, Table 5), respectively. Following the assumption that the lake is topographically closed during the LIG (zero input from the Bear River) and adopting the modern rates of the other inflow components (modern precipitation, surrounding creeks, and groundwater, Tables 1 and 4), the *X* value for the LIG translates to an evaporation rate of $1.14 \times 10^8 \pm 22\%$ m^3/yr. This is lower than the modern evaporation rate due to the combined effect of a decreased volumetric inflow because of the absence of Bear River input and presumed smaller lake surface area because of the dry, evaporative conditions during the LIG (Bright et al., 2006; Kaufman et al., 2009). Meanwhile, the *X* value during the LGP translates to an evaporation rate of $6.85 \times 10^7 \pm 17\%$ m^3/yr, an order of magnitude lower than the current rate. For this calculation, the modern inflow rate through the inlet canal was incorporated to simulate input from the Bear River, which was connected to the Bear Lake at around 40 kyr ago due to its larger surface area as suggested by surficial deposits north of the lake (Bright et al., 2006; Kaufman et al., 2009; Laabs & Kaufman, 2003). The cooler temperatures, despite being drier than the modern, might have accounted for the lower evaporation rate (Bright et al., 2006; Kaufman et al., 2009).

A mean *X* value of 0.36 ± 0.04 is derived for the future warming scenario, slightly lower than the current *X*. This slight change suggests that *X* is reasonably maintained should the isotopic composition of the inflow, particularly from the Bear River, remain constant in the future. However, a warmer and drier scenario likely corresponds to an isotopically heavier lake water, similar to the LIG. To exceed the modern *X* value in this scenario, the mean $\delta^{18}O$ composition of the lake only needs to increase by ~0.37‰. This can be estimated by using the equation of a fitted line in Figure 8j and extrapolating the lake isotopic composition that corresponds to the modern *X* value (0.38).

Additionally, calculating future evaporation rates require assumptions of volumetric inflow. Studies have shown decreasing streamflow rates due to decreasing snowpack in the western United States (Gottlieb & Mankin, 2024; Hidalgo et al., 2009; Pierce et al., 2008). Thus, the potential for higher *X* values and lower inflow volume poses a significant risk to the future availability of freshwater at Bear Lake. Calculations made in this study substantiates the utility for continuous monitoring of the lake isotopic composition to observe probable changes in evaporation rates.

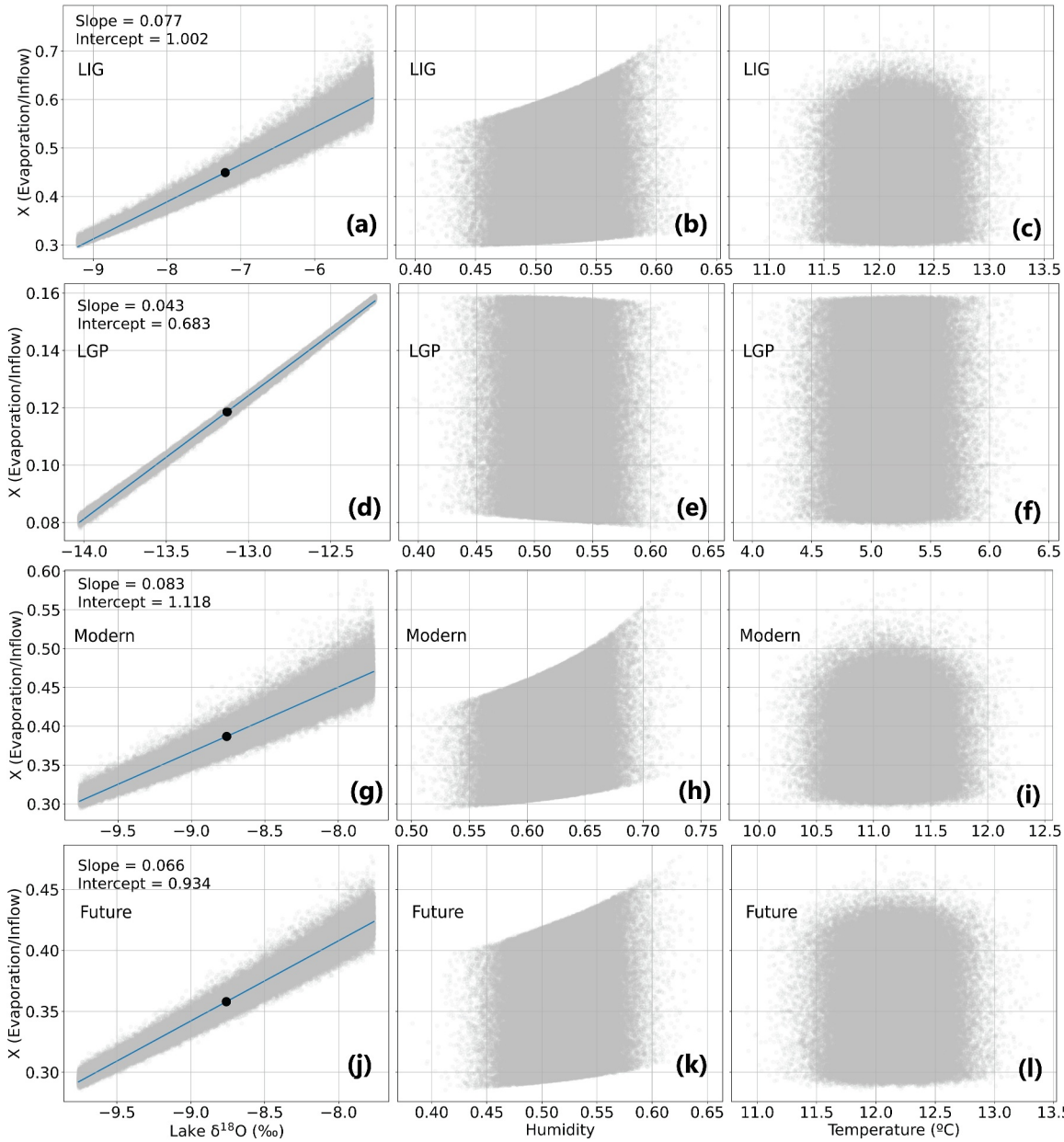

Figure 8. Simulation results ($n = 100,000$) of X with varying lake $\delta^{18}O$, humidity, and temperature (left to right panels). Panels from top to bottom correspond to LIG (a–c), LGP (d–f), modern (g–i) and future warming (j–l) scenarios. The blue lines and black markers in the leftmost panels represent the fitted regression line and the mean lake $\delta^{18}O$ and X values, respectively.

Simulating the response of X to a distribution of the three input parameters shows that, expectedly, the isotopic composition of the lake exerts significant influence based on the slopes generated from cross-plotting the two variables (Figures 8a, 8d, 8g, and 8j). Data plots for evaporation response to humidity and temperature suggest greater sensitivity to humidity, particularly at heavier lake $\delta^{18}O$ values which correspond to a higher range of X (Figures 8b, 8h, and 8k). During warmer and drier scenarios, increases in humidity corresponded to higher X values (Figures 8b, 8h, and 8k), while the LGP scenario yielded the opposite trend (Figure 8e), suggesting a slight decrease in X with increasing humidity. Figure 9 illustrates a summary cross-plot of the response of X to varying lake $\delta^{18}O$ in all climate scenarios. Figure S3 in Supporting Information S1 provides the summary cross-plots for X, humidity, and temperature. It is important to note that the observed trends are the result of simultaneously varying the three input parameters (lake $\delta^{18}O$, humidity, and temperature), obscuring the direct influence of just

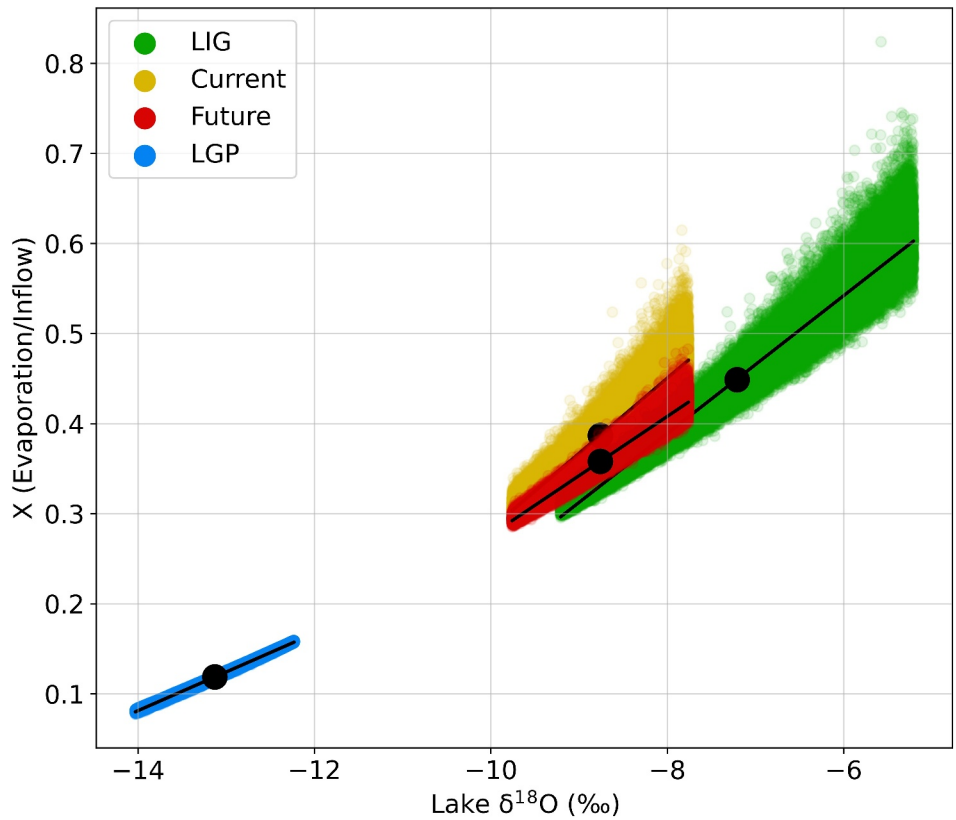

Figure 9. Summary plot of the simulation results ($n = 100,000$) of X with varying lake $\delta^{18}O$ for the four scenarios. The black lines and markers represent the fitted regression line and the mean lake $\delta^{18}O$ and X values, respectively.

humidity. Reasonable assumptions of other parameters, particularly the isotopic composition and volumetric rate of total inflow and precipitation, can yield evaporation estimates with narrower uncertainties.

7. Conclusions

The calculations and discussions presented in this study examined the water isotope systematics associated with the evaporation process at Bear Lake. Leveraging the wealth of data available in the Bear River watershed, we employed a dual-isotope ($\delta^{18}O$ and $\delta^{2}H$) approach to construct the mass balance of the lake. By simultaneously constraining the mass balances of two isotope systems, we derived values for unknown fluxes, such as evaporation and groundwater discharge, as well as the humidity above the lake that fulfills the mass balance.

Based on the findings of this paper, monthly isotopic analysis of lake water and surrounding streams can be a useful monitoring scheme to track annual changes in inflow and outflow rates. This is particularly important for mid-sized lakes in temperate regions such as the Great Basin where evaporation is highly seasonal. Furthermore, we demonstrated how isotopic mass balance models can be used to inform different climate scenarios based on available proxy data. Leveraging the sensitivity of the mass balance model to variabilities in humidity and isotopic inputs, we show that constructing the isotopic mass balance of a lake can be a useful tool in constraining past, present, and future hydrological processes within a watershed.

However, the systematics of stable isotope fractionation during evaporation are complex and caution must be used as assumptions related to the environmental conditions above a lake are critical in the calculations. Incorporating triple oxygen measurements ($\Delta^{17}O$, $\delta^{17}O$) can give more robust estimates for evaporation and groundwater fluxes. Additionally, the development of new techniques for measuring the isotopic composition of atmospheric moisture in situ could aid in narrowing the associated uncertainties. Expanding efforts in monitoring the isotopic composition of waters within a watershed is a relatively inexpensive and efficient technique that can greatly complement existing methods for water resource management.

Data Availability Statement

The hydrological data sets used for this study were compiled from monitoring stations maintained by the United States Geological Survey (USGS) and Utah Department of Environmental Quality obtained through the National Water Quality Monitoring Council Water Quality Portal (https://www.waterqualitydata.us/). A significant portion of the isotopic data set used was retrieved from the WaterIsotopes community database (https://wateriso.utah.edu/waterisotopes/). The compiled data set can be accessed through the GitHub link provided in the Supplemental data section (BL_master_list.csv). Climate data were extracted from the North American Region Reanalysis (NARR) data set produced by the NOAA National Center for Atmospheric Prediction (NCEP) (https://psl.noaa.gov/data/gridded/data.narr.html). Temperature data came from the National Weather Service (NWS) website based on a measuring station at the Lifton pump in Idaho (https://www.ncdc.noaa.gov/cdo-web/).

Acknowledgments
This research was supported by the National Science Foundation Paleo Perspectives on Climate Change (NSF—P2C2) grant (AGS 2102901 to Ibarra, AGS 2102884 to Oster, and AGS 2102885 to Sharp). We would like to acknowledge Richard Bradshaw from Vanderbilt University (2022 samples) and Anna Waldeck from the Cobb Lab at Brown University (2023 samples) for their help in analyzing the water samples collected from the field, as well as Alberto Saal, Laurence Smith, and Linda Abriola for insightful discussions.

References

Adrian, R., O'Reilly, C. M., Zagarese, H., Baines, S. B., Hessen, D. O., Keller, W., et al. (2009). Lakes as sentinels of climate change. *Limnology & Oceanography*, *54*(6part2), 2283–2297. https://doi.org/10.4319/lo.2009.54.6_part_2.2283

Amayreh, J. (1995). *Lake evaporation: A model study*. Utah State University.

Barbieri, M., Barberio, M. D., Banzato, F., Billi, A., Boschetti, T., Franchini, S., et al. (2023). Climate change and its effect on groundwater quality. *Environmental Geochemistry and Health*, *45*(4), 1133–1144. https://doi.org/10.1007/s10653-021-01140-5

Barnett, T. P., Adam, J. C., & Lettenmaier, D. P. (2005). Potential impacts of a warming climate on water availability in snow-dominated regions. *Nature*, *438*(7066), 303–309. https://doi.org/10.1038/nature04141

Berger, A. (1978). Long-term variations of daily insolation and quaternary climatic changes. *Journal of the Atmospheric Sciences*, *35*(12), 2362–2367. https://doi.org/10.1175/1520-0469(1978)035<2362:LTVODI>2.0.CO;2

Bowen, G. J. (2017). The online isotopes in precipitation calculator, version 3.1 [Dataset]. http://www.waterisotopes.org

Bowen, G. J., Cai, Z., Fiorella, R. P., & Putman, A. L. (2019). Isotopes in the water cycle: Regional-to global-scale patterns and applications. *Annual Review of Earth and Planetary Sciences*, *47*(1), 453–479. https://doi.org/10.1146/annurev-earth-053018-060220

Bowen, G. J., & Good, S. P. (2015). Incorporating water isoscapes in hydrological and water resource investigations. *WIREs Water*, *2*(2), 107–119. https://doi.org/10.1002/wat2.1069

Bowen, G. J., & Revenaugh, J. (2003). Interpolating the isotopic composition of modern meteoric precipitation. *Water Resources Research*, *39*(10), 2003WR002086. https://doi.org/10.1029/2003WR002086

Bowen, G. J., Wassenaar, L. I., & Hobson, K. A. (2005). Global application of stable hydrogen and oxygen isotopes to wildlife forensics. *Oecologia*, *143*(3), 337–348. https://doi.org/10.1007/s00442-004-1813-y

Braconnot, P., Harrison, S. P., Kageyama, M., Bartlein, P. J., Masson-Delmotte, V., Abe-Ouchi, A., et al. (2012). Evaluation of climate models using palaeoclimatic data. *Nature Climate Change*, *2*(6), 417–424. https://doi.org/10.1038/nclimate1456

Bright, J. (2009). Isotope and major-ion chemistry of groundwater in Bear Lake Valley, Utah and Idaho, with emphasis on the Bear River Range. In J. G. Rosenbaum & D. S. Kaufman (Eds.), *Paleoenvironments of Bear Lake, Utah and Idaho, and its catchment*. Geological Society of America. https://doi.org/10.1130/2009.2450(04)

Bright, J., Kaufman, D. S., Forester, R. M., & Dean, W. E. (2006). A continuous 250,000yr record of oxygen and carbon isotopes in ostracode and bulk-sediment carbonate from Bear Lake, Utah-Idaho. *Quaternary Science Reviews*, *25*(17–18), 2258–2270. https://doi.org/10.1016/j.quascirev.2005.12.011

Brooks, J. R. (2014). National rivers and streams assessment 2013–2014, 2008–2009 [Dataset]. https://wateriso.utah.edu/waterisotopes/index.html:WaterIsotopes

Brooks, J. R., Gibson, J. J., Birks, S. J., Weber, M. H., Rodecap, K. D., & Stoddard, J. L. (2014). Stable isotope estimates of evaporation: Inflow and water residence time for lakes across the United States as a tool for national lake water quality assessments. *Limnology and Oceanography*, *59*(6), 2150–2165. https://doi.org/10.4319/lo.2014.59.6.2150

Brutsaert, W. (1975). A theory for local evaporation (or heat transfer) from rough and smooth surfaces at ground level. *Water Resources Research*, *11*(4), 543–550. https://doi.org/10.1029/WR011i004p00543

Bush, A. B. G., & Philander, S. G. H. (1999). The climate of the last glacial maximum: Results from a coupled atmosphere-ocean general circulation model. *Journal of Geophysical Research*, *104*(D20), 24509–24525. https://doi.org/10.1029/1999JD900447

Cantonati, M., Poikane, S., Pringle, C. M., Stevens, L. E., Turak, E., Heino, J., et al. (2020). Characteristics, main impacts, and stewardship of natural and artificial freshwater environments: Consequences for biodiversity conservation. *Water*, *12*(1), 260. https://doi.org/10.3390/w12010260

Colman, S. M., Kaufman, D. S., Bright, J., Heil, C., King, J. W., Dean, W. E., et al. (2006). Age model for a continuous, ca 250-ka Quaternary lacustrine record from Bear Lake, Utah–Idaho. *Quaternary Science Reviews*, *25*(17–18), 2271–2282. https://doi.org/10.1016/j.quascirev.2005.10.015

Colman, S. M., Rosenbaum, J. G., Kaufman, D. S., Dean, W. E., & McGeehin, J. P. (2009). Radiocarbon ages and age models for the past 30,000 years in Bear Lake, Utah and Idaho. In J. G. Rosenbaum & D. S. Kaufman (Eds.), *Paleoenvironments of Bear Lake, Utah and Idaho, and its catchment*. Geological Society of America. https://doi.org/10.1130/2009.2450(05)

Cooley, S. W., Ryan, J. C., & Smith, L. C. (2021). Human alteration of global surface water storage variability. *Nature*, *591*(7848), 78–81. https://doi.org/10.1038/s41586-021-03262-3

Coplen, T. B., Kendall, C., & Hopple, J. (1983). Comparison of stable isotope reference samples. *Nature*, *302*(5905), 236–238. https://doi.org/10.1038/302236a0

Craig, H., & Gordon, L. (1965). Deuterium and oxygen 18 variations in the ocean and marine atmosphere. Retrieved from https://www.semanticscholar.org/paper/Deuterium-and-oxygen-18-variations-in-the-ocean-and-Craig-Gordon/b803d3615c35b9c25d19fe88afd354f08368c085

Dean, W. E., Rosenbaum, J., Skipp, G., Colman, S., Forester, R., Liu, A., et al. (2006). Unusual holocene and late pleistocene carbonate sedimentation in Bear Lake, Utah and Idaho, USA. *Sedimentary Geology*, *185*(1–2), 93–112. https://doi.org/10.1016/j.sedgeo.2005.11.016

Dean, W. E. (2009). Endogenic carbonate sedimentation in Bear Lake, Utah and Idaho, over the last two glacial-interglacial cycles. In J. G. Rosenbaum & D. S. Kaufman (Eds.), *Paleoenvironments of Bear Lake, Utah and Idaho, and its catchment*. Geological Society of America. https://doi.org/10.1130/2009.2450(07)

Dean, W. E., Forester, R. M., Bright, J., & Anderson, R. Y. (2007). Influence of the diversion of Bear River into Bear Lake (Utah and Idaho) on the environment of deposition of carbonate minerals. *Limnology & Oceanography*, *52*(3), 1094–1111. https://doi.org/10.4319/lo.2007.52.3.1094

Dean, W. E., Wurtsbaugh, W. A., & Lamarra, V. A. (2009). Climatic and limnologic setting of Bear Lake, Utah and Idaho. In J. G. Rosenbaum & D. S. Kaufman (Eds.), *Paleoenvironments of Bear Lake, Utah and Idaho, and its catchment*. Geological Society of America. https://doi.org/10.1130/2009.2450(01)

Dee, S., Bailey, A., Conroy, J. L., Atwood, A., Stevenson, S., Nusbaumer, J., & Noone, D. (2023). Water isotopes, climate variability, and the hydrological cycle: Recent advances and new frontiers. *Environmental Research: Climate*, *2*(2), 022002. https://doi.org/10.1088/2752-5295/accbe1

De Wet, C. B., Ibarra, D. E., Belanger, B. K., & Oster, J. L. (2023). North American hydroclimate during past warms states: A proxy compilation-model comparison for the last interglacial and the mid-holocene. *Paleoceanography and Paleoclimatology*, *38*(6), e2022PA004528. https://doi.org/10.1029/2022PA004528

Dudgeon, D., Arthington, A. H., Gessner, M. O., Kawabata, Z.-I., Knowler, D. J., Lévêque, C., et al. (2006). Freshwater biodiversity: Importance, threats, status and conservation challenges. *Biological Reviews*, *81*(2), 163–182. https://doi.org/10.1017/S1464793105006950

Dutton, A., & Lambeck, K. (2012). Ice volume and sea level during the last interglacial. *Science*, *337*(6091), 216–219. https://doi.org/10.1126/science.1205749

Felis, T., Giry, C., Scholz, D., Lohmann, G., Pfeiffer, M., Pätzold, J., et al. (2015). Tropical Atlantic temperature seasonality at the end of the last interglacial. *Nature Communications*, *6*(1), 6159. https://doi.org/10.1038/ncomms7159

Fiorella, R. (2012). Survey of NW Wyoming surface waters [Dataset]. https://wateriso.utah.edu/waterisotopes/index.html:WaterIsotopes

Friedman, I., Smith, G. I., Johnson, C. A., & Moscati, R. J. (2002). Stable isotope compositions of waters in the Great Basin, United States 2. Modern precipitation. *Journal of Geophysical Research*, *107*(D19), ACL15-1–ACL15-22. https://doi.org/10.1029/2001JD000566

Gat, J. R. (1995). Stable isotopes of fresh and saline lakes. In A. Lerman, D. M. Imboden, & J. R. Gat (Eds.), *Physics and chemistry of lakes* (pp. 139–165). Springer. https://doi.org/10.1007/978-3-642-85132-2_5

Gibson, J. J., Birks, S. J., & Edwards, T. W. D. (2008). Global prediction of δ A and δ^2H-δ^{18}O evaporation slopes for lakes and soil water accounting for seasonality. *Global Biogeochemical Cycles*, *22*(2), 2007GB002997. https://doi.org/10.1029/2007GB002997

Gibson, J. J., Birks, S. J., & Moncur, M. (2019). Mapping water yield distribution across the South Athabasca Oil Sands (SAOS) area: Baseline surveys applying isotope mass balance of lakes. *Journal of Hydrology: Regional Studies*, *21*, 1–13. https://doi.org/10.1016/j.ejrh.2018.11.001

Gibson, J. J., Birks, S. J., & Yi, Y. (2016). Stable isotope mass balance of lakes: A contemporary perspective. *Quaternary Science Reviews*, *131*, 316–328. https://doi.org/10.1016/j.quascirev.2015.04.013

Gibson, J. J., Birks, S. J., Yi, Y., Moncur, M. C., & McEachern, P. M. (2016). Stable isotope mass balance of fifty lakes in central Alberta: Assessing the role of water balance parameters in determining trophic status and lake level. *Journal of Hydrology: Regional Studies*, *6*, 13–25. https://doi.org/10.1016/j.ejrh.2016.01.034

Gibson, J. J., Edwards, T. W. D., Bursey, G. G., & Prowse, T. D. (1993). Estimating evaporation using stable isotopes: Quantitative results and sensitivity analysis for two catchments in northern Canada. *Hydrology Research*, *24*(2–3), 79–94. https://doi.org/10.2166/nh.1993.0015

Gonfiantini, R. (1986). Environmental isotopes in lake studies. In *The terrestrial environment, B* (pp. 113–168). Elsevier. https://doi.org/10.1016/B978-0-444-42225-5.50008-5

Gonfiantini, R., Wassenaar, L. I., Araguas-Araguas, L., & Aggarwal, P. K. (2018). A unified Craig-Gordon isotope model of stable hydrogen and oxygen isotope fractionation during fresh or saltwater evaporation. *Geochimica et Cosmochimica Acta*, *235*, 224–236. https://doi.org/10.1016/j.gca.2018.05.020

Gonfiantini, R., Wassenaar, L. I., & Araguas-Araguas, L. J. (2020). Stable isotope fractionations in the evaporation of water: The wind effect. *Hydrological Processes*, *34*(16), 3596–3607. https://doi.org/10.1002/hyp.13804

Gottlieb, A. R., & Mankin, J. S. (2024). Evidence of human influence on Northern Hemisphere snow loss. *Nature*, *625*(7994), 293–300. https://doi.org/10.1038/s41586-023-06794-y

Gronewold, A. D., Smith, J. P., Read, L. K., & Crooks, J. L. (2020). Reconciling the water balance of large lake systems. *Advances in Water Resources*, *137*, 103505. https://doi.org/10.1016/j.advwatres.2020.103505

Haig, H. A., Hayes, N. M., Simpson, G. L., Yi, Y., Wissel, B., Hodder, K. R., & Leavitt, P. R. (2020). Comparison of isotopic mass balance and instrumental techniques as estimates of basin hydrology in seven connected lakes over 12 years. *Journal of Hydrology X*, *6*, 100046. https://doi.org/10.1016/j.hydroa.2019.100046

Henderson-Sellers, B. (1986). Calculating the surface energy balance for lake and reservoir modeling: A review. *Reviews of Geophysics*, *24*(3), 625–649. https://doi.org/10.1029/RG024i003p00625

Herman, J., & Usher, W. (2017). SALib: An open-source Python library for sensitivity analysis. *Journal of Open Source Software*, *2*(9), 97. https://doi.org/10.21105/joss.00097

Hidalgo, H. G., Das, T., Dettinger, M. D., Cayan, D. R., Pierce, D. W., Barnett, T. P., et al. (2009). Detection and attribution of streamflow timing changes to climate change in the western United States. *Journal of Climate*, *22*(13), 3838–3855. https://doi.org/10.1175/2009JCLI2470.1

Horita, J., Rozanski, K., & Cohen, S. (2008). Isotope effects in the evaporation of water: A status report of the Craig–Gordon model. *Isotopes in Environmental and Health Studies*, *44*(1), 23–49. https://doi.org/10.1080/10256010801887174

Horita, J., & Wesolowski, D. J. (1994). Liquid-vapor fractionation of oxygen and hydrogen isotopes of water from the freezing to the critical temperature. *Geochimica et Cosmochimica Acta*, *58*(16), 3425–3437. https://doi.org/10.1016/0016-7037(94)90096-5

IAEA/WMO. (2015). Global network of isotopes in precipitation [Dataset]. *The GNIP Database*. Retrieved from https://www.iaea.org/services/networks/gnip

Idaho Department of Water. (2015). ID groundwater quality database (EDMS) [Dataset]. Retrieved from https://wateriso.utah.edu/waterisotopes/index.html:WaterIsotopes

Iwanaga, T., Usher, W., & Herman, J. (2022). Toward SALib 2.0: Advancing the accessibility and interpretability of global sensitivity analyses. *Socio-Environmental Systems Modelling*, *4*, 18155. https://doi.org/10.18174/sesmo.18155

Jasechko, S. (2019). Global isotope hydrogeology——Review. *Reviews of Geophysics*, *57*(3), 835–965. https://doi.org/10.1029/2018RG000627

Jasechko, S., Gibson, J. J., & Edwards, T. W. D. (2014). Stable isotope mass balance of the Laurentian Great Lakes. *Journal of Great Lakes Research*, *40*(2), 336–346. https://doi.org/10.1016/j.jglr.2014.02.020

Jones, M. D., Roberts, C. N., & Leng, M. J. (2007). Quantifying climatic change through the last glacial–interglacial transition based on lake isotope palaeohydrology from central Turkey. *Quaternary Research*, *67*(3), 463–473. https://doi.org/10.1016/j.yqres.2007.01.004

Kaliser, B. N. (1972). *Environmental Geology of Bear Lake area, rich County_Utah*. UtahGeological and Mineralogical Survey. Retrieved from https://ugspub.nr.utah.gov/publications/bulletins/b-96.pdf

Kaufman, D. S., Bright, J., Dean, W. E., Rosenbaum, J. G., Moser, K., Anderson, R. S., et al. (2009). A quarter-million years of paleoenvironmental change at Bear Lake, Utah and Idaho. In J. G. Rosenbaum & D. S. Kaufman (Eds.), *Paleoenvironments of Bear Lake, Utah and Idaho, and its catchment*. Geological Society of America. https://doi.org/10.1130/2009.2450(14)

Kendall, C. (1987). Tracking water-quality of the national rivers and streams [Dataset]. Retrieved from https://wateriso.utah.edu/waterisotopes/index.html:WaterIsotopes

Kukla, G. J., Bender, M. L., de Beaulieu, J.-L., Bond, G., Broecker, W. S., Cleveringa, P., et al. (2002). Last interglacial climates. *Quaternary Research*, *58*(1), 2–13. https://doi.org/10.1006/qres.2001.2316

Laabs, B. J. C., & Kaufman, D. S. (2003). Quaternary highstands in Bear Lake Valley, Utah and Idaho. *Geological Society of America Bulletin*, *115*, 463–478. https://doi.org/10.1130/0016-7606(2003)115<0463:QHIBLV>2.0.CO;2

Laabs, B. J. C., Munroe, J. S., Rosenbaum, J. G., Refsnider, K. A., Mickelson, D. M., Singer, B. S., & Caffee, M. W. (2007). Chronology of the last glacial maximum in the upper Bear River basin, Utah. *Arctic Antarctic and Alpine Research*, *39*(4), 537–548. https://doi.org/10.1657/1523-0430(06-089)[LAABS]2.0.CO;2

Lamarra, V., Liff, C., & Carter, J. (1986). Hydrology of Bear Lake basin and its impact on the trophic state of Bear Lake, Utah-Idaho. *Great Basin Naturalist*, *46*(4), 690–705.

Longinelli, A., Stenni, B., Genoni, L., Flora, O., Defrancesco, C., & Pellegrini, G. (2008). A stable isotope study of the Garda lake, northern Italy: Its hydrological balance. *Journal of Hydrology*, *360*(1–4), 103–116. https://doi.org/10.1016/j.jhydrol.2008.07.020

Lunt, D. J., Abe-Ouchi, A., Bakker, P., Berger, A., Braconnot, P., Charbit, S., et al. (2013). A multi-model assessment of last interglacial temperatures. *Climate of the Past*, *9*(2), 699–717. https://doi.org/10.5194/cp-9-699-2013

Merlivat, L. (1978). Molecular diffusivities of H2 16O, HD16O, and H2 18O in gases. *The Journal of Chemical Physics*, *69*(6), 2864–2871. https://doi.org/10.1063/1.436884

Mesinger, F., DiMego, G., Kalnay, E., Mitchell, K., Shafran, P. C., Ebisuzaki, W., et al. (2006). North American regional reanalysis. *Bulletin of the American Meteorological Society*, *87*(3), 343–360. https://doi.org/10.1175/BAMS-87-3-343

National Water Quality Monitoring Council. (2021). Water quality portal [Dataset]. https://doi.org/10.5066/P9QRKUVJ

O'Neil, J. R., Clayton, R. N., & Mayeda, T. K. (1969). Oxygen isotope fractionation in divalent metal carbonates. *The Journal of Chemical Physics*, *51*(12), 5547–5558. https://doi.org/10.1063/1.1671982

PacifiCorp. (2019). *Lifton fact sheet*. PacifiCorp. Retrieved from https://legislature.idaho.gov/wp-content/uploads/sessioninfo/2016/interim/160923_iswg_07_VAUGHNLiftonFactSheet.pdf

Passey, B. H., & Ji, H. (2019). Triple oxygen isotope signatures of evaporation in lake waters and carbonates: A case study from the western United States. *Earth and Planetary Science Letters*, *518*, 1–12. https://doi.org/10.1016/j.epsl.2019.04.026

Picarro. (2024). L2130-i isotope and gas concentration analyzer | Picarro. Retrieved from https://www.picarro.com/environmental/products/l2130i_isotope_and_gas_concentration_analyzer

Pierce, D. W., Barnett, T. P., Hidalgo, H. G., Das, T., Bonfils, C., Santer, B. D., et al. (2008). Attribution of declining western U.S. snowpack to human effects. *Journal of Climate*, *21*(23), 6425–6444. https://doi.org/10.1175/2008JCLI2405.1

Pierchala, A., Rozanski, K., Dulinski, M., & Gorczyca, Z. (2022). Quantification the diffusion-induced fractionation of $^{1}H_{2}{}^{17}O$ isotopologue in air accompanying the process of water evaporation. *Geochimica et Cosmochimica Acta*, *322*, 244–259. https://doi.org/10.1016/j.gca.2022.01.020

Powell, M. J. D. (1970). A hybrid method for nonlinear equations. In P. Rabinowitz (Ed.), *Numerical methods for nonlinear algebraic equations*. Gordon and Breach.

Rosenbaum, J. G., Reynolds, R. L., & Colman, S. M. (2012). Fingerprinting of glacial silt in lake sediments yields continuous records of alpine glaciation (35–15 ka), western USA. *Quaternary Research*, *78*(2), 333–340. https://doi.org/10.1016/j.yqres.2012.06.004

Russell, J. M., & Johnson, T. C. (2006). The water balance and stable isotope hydrology of Lake Edward, Uganda-Congo. *Journal of Great Lakes Research*, *32*(1), 77–90. https://doi.org/10.3394/0380-1330(2006)32[77:TWBASI]2.0.CO;2

Schindler, D. E., & Scheuerell, M. D. (2002). Habitat coupling in lake ecosystems. *Oikos*, *98*(2), 177–189. https://doi.org/10.1034/j.1600-0706.2002.980201.x

Shackleton, S., Baggenstos, D., Menking, J. A., Dyonisius, M. N., Bereiter, B., Bauska, T. K., et al. (2020). Global ocean heat content in the Last Interglacial. *Nature Geoscience*, *13*(1), 77–81. https://doi.org/10.1038/s41561-019-0498-0

Sharan, A., Lal, A., & Datta, B. (2023). Evaluating the impacts of climate change and water over-abstraction on groundwater resources in Pacific island country of Tonga. *Groundwater for Sustainable Development*, *20*, 100890. https://doi.org/10.1016/j.gsd.2022.100890

Steinman, B. A., Rosenmeier, M. F., & Abbott, M. B. (2010). The isotopic and hydrologic response of small, closed-basin lakes to climate forcing from predictive models: Simulations of stochastic and mean state precipitation variations. *Limnology & Oceanography*, *55*(6), 2246–2261. https://doi.org/10.4319/lo.2010.55.6.2246

Steinman, B. A., Rosenmeier, M. F., Abbott, M. B., & Bain, D. J. (2010). The isotopic and hydrologic response of small, closed-basin lakes to climate forcing from predictive models: Application to paleoclimate studies in the upper Columbia River basin. *Limnology & Oceanography*, *55*(6), 2231–2245. https://doi.org/10.4319/lo.2010.55.6.2231

Suh, Y. J., Diefendorf, A. F., Freimuth, E. J., & Hyun, S. (2020). Last interglacial (MIS 5e) and Holocene paleohydrology and paleovegetation of midcontinental North America from Gulf of Mexico sediments. *Quaternary Science Reviews*, *227*, 106066. https://doi.org/10.1016/j.quascirev.2019.106066

Terrazas, A., Hwangbo, N., Arnold, A. J., Ulrich, R. N., & Tripati, A. (2023). Seasonal lake-to-air temperature transfer functions derived from an analysis of 965 modern lakes: A tool for lacustrine proxy model comparison. https://doi.org/10.22541/essoar.169945141.15177214/v1

Tierney, J. E., Zhu, J., King, J., Malevich, S. B., Hakim, G. J., & Poulsen, C. J. (2020). Glacial cooling and climate sensitivity revisited. *Nature*, *584*(7822), 569–573. https://doi.org/10.1038/s41586-020-2617-x

U.S. Geological Survey. (2008). Temperature. In F. Wilde (Eds.), *Chapter A6. Field measurements: Techniques of water-resources investigations 09-A6* (pp. T3–T22). U.S. Geological Survey. Retrieved from https://pubs.usgs.gov/twri/twri9a6/twri9a6_6.1_ver2.pdf

U.S. Geological Survey. (2024). National water information system data [Dataset]. https://doi.org/10.5066/F7P55KJN

Utah Geological Survey. (2017). Ogden Valley water [Dataset]. Retrieved from https://wateriso.utah.edu/waterisotopes/index.html:WaterIsotopes

Virtanen, P., Gommers, R., Oliphant, T. E., Haberland, M., Reddy, T., Cournapeau, D., et al. (2020). SciPy 1.0: Fundamental algorithms for scientific computing in Python. *Nature Methods*, *17*(3), 261–272. https://doi.org/10.1038/s41592-019-0686-2

Vystavna, Y., Harjung, A., Monteiro, L. R., Matiatos, I., & Wassenaar, L. I. (2021). Stable isotopes in global lakes integrate catchment and climatic controls on evaporation. *Nature Communications*, *12*(1), 7224. https://doi.org/10.1038/s41467-021-27569-x

Wang, W., Lee, X., Xiao, W., Liu, S., Schultz, N., Wang, Y., et al. (2018). Global lake evaporation accelerated by changes in surface energy allocation in a warmer climate. *Nature Geoscience*, *11*(6), 410–414. https://doi.org/10.1038/s41561-018-0114-8

WaterIsotopes Database. (2017). [Dataset]. Retrieved from http://waterisotopesDB.org

Welker, J. M. (2000). Isotopic (δ18O) characteristics of weekly precipitation collected across the USA: An initial analysis with application to water source studies. *Hydrological Processes*, *14*(8), 1449–1464. https://doi.org/10.1002/1099-1085(20000615)14:8<1449::AID-HYP993>3.0.CO;2-7

Woolway, R. I., Kraemer, B. M., Lenters, J. D., Merchant, C. J., O'Reilly, C. M., & Sharma, S. (2020). Global lake responses to climate change. *Nature Reviews Earth and Environment*, *1*(8), 388–403. https://doi.org/10.1038/s43017-020-0067-5

Wurtsbaugh, W. A., Miller, C., Null, S. E., DeRose, R. J., Wilcock, P., Hahnenberger, M., et al. (2017). Decline of the world's saline lakes. *Nature Geoscience*, *10*(11), 816–821. https://doi.org/10.1038/ngeo3052

Xiao, W., Lee, X., Hu, Y., Liu, S., Wang, W., Wen, X., et al. (2017). An experimental investigation of kinetic fractionation of open-water evaporation over a large lake. *Journal of Geophysical Research: Atmospheres*, *122*(21), 11651–11663. https://doi.org/10.1002/2017JD026774

Xie, C., Xiao, W., Zhang, M., Liu, S., Qian, Y., Zhu, H., et al. (2021). Isotopic kinetic fractionation of evaporation from small water bodies. *Journal of Hydrology*, *603*, 126974. https://doi.org/10.1016/j.jhydrol.2021.126974

Yi, Y., Brock, B. E., Falcone, M. D., Wolfe, B. B., & Edwards, T. W. D. (2008). A coupled isotope tracer method to characterize input water to lakes. *Journal of Hydrology*, *350*(1–2), 1–13. https://doi.org/10.1016/j.jhydrol.2007.11.008

Yin, X., & Nicholson, S. E. (1998). The water balance of Lake Victoria. *Hydrological Sciences Journal*, *43*(5), 789–811. https://doi.org/10.1080/02626669809492173

Yusuf, J. (2013). Utah water survey [Dataset]. Retrieved from https://wateriso.utah.edu/waterisotopes/index.html:WaterIsotopes

Zannoni, D., Steen-Larsen, H. C., Peters, A. J., Wahl, S., Sodemann, H., & Sveinbjörnsdóttir, A. E. (2022). Non-equilibrium fractionation factors for D/H and $^{18}O/^{16}O$ during oceanic evaporation in the North-West Atlantic region. *Journal of Geophysical Research: Atmospheres*, *127*(21), e2022JD037076. https://doi.org/10.1029/2022JD037076

Zhao, B., Huntington, J., Pearson, C., Zhao, G., Ott, T., Zhu, J., et al. (2024). Developing a general daily lake evaporation model and demonstrating its application in the State of Texas. *Water Resources Research*, *60*(3), e2023WR036181. https://doi.org/10.1029/2023WR036181

Zhao, G., & Gao, H. (2019). Estimating reservoir evaporation losses for the United States: Fusing remote sensing and modeling approaches. *Remote Sensing of Environment*, *226*, 109–124. https://doi.org/10.1016/j.rse.2019.03.015

Zhao, G., Li, Y., Zhou, L., & Gao, H. (2022). Evaporative water loss of 1.42 million global lakes. *Nature Communications*, *13*(1), 3686. https://doi.org/10.1038/s41467-022-31125-6